UNIVERSIDADE DOS AÇORES

DEPARTAMENTO DE OCEANOGRAFIA E PESCAS

Relatório de Estágio
Licenciatura em Biologia Marinha
do Departamento de Biologia

Sea Surface Temperature (SST) and Ocean Color (OC) pattern relationships on an annual and seasonal basis in the Subtropical NE Atlantic, using satellite (AVHRR and MODIS) data (2002-2006).

Comparação de padrões anuais e sazonais da temperatura de superfície (SST) e côr do oceano (OC) no Atlântico NE Subtropical, com a utilização de dados (2002-2006) satélite AVHRR e MODIS.

João Vieira Santos Mesquita Guimarães

HORTA
-2008-

UNIVERSIDADE DOS AÇORES

DEPARTAMENTO DE OCEANOGRAFIA E PESCAS

Relatório de Estágio
Licenciatura em Biologia Marinha
do Departamento de Biologia

Sea Surface Temperature (SST) and Ocean Color (OC) pattern relationships on an annual and seasonal basis in the Subtropical NE Atlantic, using satellite (AVHRR and MODIS) data (2002-2006).

Comparação de padrões anuais e sazonais da temperatura de superfície (SST) e côr do oceano (OC) no Atlântico NE Subtropical, com a utilização de dados (2002-2006) satélite AVHRR e MODIS.

Por:

João Vieira Santos Mesquita Guimarães

Supervisor:

Ana Maria de Pinho Ferreira de Silva Fernandes Martins (DOP/UAç)

Orientador:

Igor Bashmachnikov (IMAR-DOP/UAç)

HORTA
-2008-

Table of Contents

List of Tables

List of Figures

Abstract

Main objectives of this study are to describe temporal and spatial variability of sea surface temperature (SST) and Ocean Color (OC) in the Subtropical Atlantic on monthly, seasonal and inter-annual scales. As an input, five years (2002-2006) of AVHRR SST (in ºC) (NASA/JPL/PO.DACC) and of MODIS OC (chlorophyll *a* in mg/ m^3) (NASA/GSFC) images were used. At the south-western part of the region, the ocean waters were generally the warmest, while the highest OC was found at the Portuguese coast. Result show that SST variability in the region is primarily a balance between ocean surface heating and wind mixing, with some input of SST gradients transport by advection. In tropical waters, inter-annual SST variability showed high negative correlations with NAO index. With some exceptions, Ocean Color seasonal variability varied inversely with respect to SST. In the open ocean regions spring bloom produced the highest chlorophyll *a* concentration while at the Portuguese coast strong summer bloom is present. In tropical regions, OC variability showed significant negative correlations with SST, particularly during spring and summer.

Keywords: Northeast Subtropical Atlantic, temporal variability, sea surface temperature, ocean color.

Resumo

Os principais objectivos deste estudo são descrever a variabilidade espacial e temporal da temperatura de superficie do mar (SST) e da Cor do Oceano (OC) no Atlântico Subtropical a uma escala mensal, sazonal e anual. Foram usadas cinco anos (2002-2006) de imagens AVHRR SST (em ºC) (NASA/JPL/PO.DAAC) e MODIS OC (clorofila a em mg/ m^3) (NASA/GSFC). A parte sudoeste da região foi geralmente a mais quente enquanto os valores mais elevados de clorofila foram encontrados na costa portuguesa. Os resultados mostram que a variabilidade de SST na região são devido a um balanço entre o aquecimento da superficie do oceano e a mistura causada pelo vento. A variabilidade inter-anual de SST mostrou correlação negativa alta com o index

da NAO. Com algumas excepções a variabilidade sazonal de OC variou inversamente no que diz respeito ao SST. Nas regiões oceanicas o bloom de Primavera produziu as concentrações de clorofila a mais elevadas enquano que na costa portguesa ocorreu um bloom de Verão forte. Nas regiões tropicais, e particularmente durante a Primavera e Verão, a variabilidade de OC mostrou uma significante correlação negativa relativamente ao SST.

Palavras chave: Atlântico Nordeste Subtropical, variabilidade temporal, temperatura de superficie do oceano, cor do oceano.

1. INTRODUCTION

The study of spatial and temporal variability of surface temperature and ocean color patterns is of much interest for both commercial (e.g. fisheries, water quality monitoring services) and research (e.g. atmospheric circulation/forecast models, estimation of primary production, coupled physical-biological interactions) points of view. For subtropical and tropical waters SST may serve as an indicator of vertical mixing in the upper ocean layer with the lower ones. For the upper ocean layer this mixing serves the major source of nutrients, which regulates plankton biomass and primary productivity in the regions. Form another side, Ocean color can be regarded as a direct measure of phytoplankton abundance and productivity in the region. There are various approaches which permit to convert the chlorophyll *a* concentration, derived from OC, to phytoplankton biomass and productivity, thus linking the former with some of the most important biological characteristics of the ocean (Longhurst, 1995).

Sea Surface Temperature (SST) and Ocean Color (OC), measured from space, provide an almost instantaneous large-scale view of related physical and biological ocean patterns. Due to its global and repeated coverage, satellite-based remote sensing offers the unique observational approach suitable for routine measurement of physical and biological properties over large regions of the ocean (McGillicuddy *et al.*, 2001). The highest quality available information on the SST and OC characteristics of the ocean can be obtained from the Advanced Very High Resolution Radiometer (AVHRR, NOAA satellites) and Moderate Resolution Imaging Spectroradiometer (MODIS, Aqua and Terra satellites) instruments. Previous investigations have documented coherence between SST and OC in several different regions of the world ocean, including the northeast Atlantic (Gower *et al.*, 1980, Martins *et al*. 2007), and the Gulf Stream (Moliner and Yoder, 1994). However, the nature of this relationship in the subtropical gyres has received less attention (McGillicuddy *et al.*, 2001), while joint analysis of SST and OC can provide an insight into physical mechanisms which govern the phytoplankton dynamics in the region.

The Azores region is characterized by rather high horizontal temperature gradients, enhanced by two eastward flows: the cold southern branch of the North Atlantic Current (NAC), and the warm Azores Current (AzC) (Bashmachnikov *et al*., 2004). The southern branch of the NAC and the AzC are most pronounced in the eastern part of

the Eastern subtropical Atlantic basin and have a slight tendency to converge towards the Iberian Peninsula (Martins *et al*. 2007). This convergence enhances meridional temperature gradients in the region. The highest horizontal temperature (1ºC per 50km) and salinity gradients in the upper layer are found in the Azores front (AzF) (Gould, 1985). This author suggested marking the frontal interface between the Subtropical and the North-East Atlantic Central waters at 18 ºC isotherm. The position of the AzF and 60-km wide jet-like AzC exhibits seasonal migrations of about 3° latitude, performing a retreat towards the south in summer and progress northward in winter (Stramma and Siedler, 1988).

Seasonal variability of phytoplankton in the region is characterized by spring bloom, summer minimum, followed by modest autumn and winter increase. Phytoplankton temporal and spatial variability in the region is deeply influenced by seasonality of physical properties and water dynamics. One of the most important regulating factors, initiating spring bloom in subtropics and winter increase in tropics is the vertical stability of the water column. From autumn to winter, the upper mixed layer depth deepens, favouring the entrainment of nutrient rich cold deep waters into the photic zone. From spring to summer the picnocline strengthens, and the upper mixed layer becomes the shallowest (10-30 m) and more effectively separated from the ocean interior (Teira *et al.*, 2005).

This investigation aims to study temporal and spatial variability of SST and OC in the Eastern Subtropical Atlantic. It is based on a comparative analysis of five years of NOAA/AVHRR and MODIS/AQUA monthly satellite imagery for 9 sub-regions. We look for statistical dependencies between SST and OC patterns and their temporal changes on monthly, seasonal and inter-annual time scales.

The following Section presents background information on the general dynamics of the region and remote sensing of SST and OC. Section 3 describes the data sets and the methodology. Section 4 presents the results. Section 5 discusses the results obtained and section 6 presents the conclusions from this study.

2. BACKGROUND

2.1. General Description of the Region of Study

The subtropical gyres are extensive, coherent regions that occupy about 40% of the surface of the ocean. Once thought to be homogeneous and static habitats, there is increasing evidence that they exhibit substantial physical and biological variability on a variety of time scales (Mclain *et al.*, 2004). While biological productivity within these oligotrophic regions may be relatively small, their immense size makes their total contribution significant (Teira *et al.*, 2005).

The Azores archipelago is located at the northern edge of the North Atlantic Subtropical Gyre (SG), considered to be the rotor of the North Atlantic circulation (Bashmachnikov *et al*., 2004). In the Azores region, the mean currents, as well as mesoscale motions, are comparatively weak (Lafon *et al*., 2004). The Gulf Stream current feeds the Azores area, entering the region as several branches. The southern branch is called the Azores current (AzC) and it crosses the Mid-Atlantic ridge (MAR) between 32° and 35 ºN (Klein & Siedler, 1989). The AzC flows across the eastern basin at approximately 34°-35ºN as jet-like meandering zonal current with three main southward recirculation branches joining at low tropics the North Equatorial Current. The northern branch, influencing temperature variability in the region, is a southern branch of the North Atlantic Current (NAC) that crosses MAR at 45-48 ºN (Bashmachnikov *et al*., 2004).

The AzC is confined to a band of strong temperature and salinity gradients, known as Azores Front (AzF), and forms the northern boundary of warm salty tropical waters (Pingree *et al*., 1999). Stramma and Siedler (1988) reported seasonal variation in the AzC-AzF position, which (south of the Azores) shifts to the south in summer as far as 2º latitude. Mesoscale variability in the Azores-Madeira region is also closely related to the meandering of the AzC-AzF system (Pingree *et al*., 1999).

2.2. Definition of Remotely Observed Sea Surface Temperature

The vertical temperature structure of the uppermost ocean (~10 m) is both complex and variable depending on the level of shear-driven ocean turbulence and the air–sea fluxes of heat, moisture, and momentum (Emery *et al*., 1995; Donlon *et al*., 2002). Every Sea Surface Temperature (SST) observation depends on the measurement technique and sensor used, the vertical position of the measurement within the water column, the local history of all component heat flux conditions, and the time of day when the measurement was obtained. Due to all these dependences, there are different concepts of SST. Definitions of SST provide a necessary theoretical framework that can be used to understand the information content and relationships between measurements of SST made by satellite and *in situ*.

The vertical structure of SST can be generally classified as follows (GHRSST-PP, 2007).

- The interface SST (SSTint) is a theoretical temperature at the precise air-sea interface and it represents the hypothetical temperature of the topmost layer of the ocean water. SSTint is of no practical use because it cannot be measured using current technology. It is important to note that it is the SSTint that interacts with the atmosphere.
- The skin SST (SSTskin) is defined as the radiometric temperature measured by an infrared radiometer operating in the 10-12 micrometer spectral waveband. As such, it represents the actual temperature of the water across a very small depth of approximately 20 micrometers. This definition is chosen for consistency with the majority of infrared satellite and ship mounted radiometer measurements. According to Donlon *et al*. (2002) a strong temperature gradient is characteristically maintained in this thin layer sustained by the magnitude and direction of the ocean–atmosphere heat flux. SSTskin measurements are subject to a large potential diurnal cycle including cool skin layer effects (especially at night under clear skies and low wind speed conditions) and warm layer effects in the daytime.
- The sub-skin SST (SSTsubskin) represents the temperature at the base of the thermal skin layer where molecular and viscous heat transfer processes begin to dominate. It is of ~1mm thick at the ocean surface. It varies on a timescale of minutes

and may be influenced by solar warming (Donlon *et al.*, 2002). For practical purposes, SSTsubskin can be derived from the measurements of surface temperature by a microwave radiometer operating in the 6-11 GHz frequency range, but the relationship is neither direct nor invariant to changing physical conditions or to the specific geometry of the microwave measurements.

- The subsurface SST, $SST_{depth,}$ (traditionally referred to as a ''bulk'' SST) considers any temperature within the water column beneath the $SST_{subskin}$ where turbulent heat transfer processes dominate. It may be significantly influenced by local solar heating and has a time scale of hours and typically varies with depth (Donlon *et al.*, 2002).

- The Foundation SST (SSTfnd) is defined as the temperature of the water column free of diurnal temperature variability or equal to the SSTsubskin in the absence of any diurnal signal. It is named to indicate that it is the foundation temperature from which the growth of the diurnal thermocline develops each day. The SSTfnd product provides an SST that is free of any diurnal variations (daytime warming or nocturnal cooling). Only *in situ* contact thermometry is able to measure SSTfnd. Analysis procedures must be used to estimate the SSTfnd from radiometric measurements of SSTskin and SSTsubskin (GHRSST-PP, 2007).

Thus, without a clear statement of the precise depth at which the SST measurement was made, and the circumstances surrounding the measurement, such a sample lacks the information needed for comparison with, or validation of satellite-derived estimates of SST using other data sources. All measurements of water temperature, obtained from a wide variety of sensors such as drifting buoys, moored buoys, thermosalinograph (TSG) systems, Conductivity Temperature and Depth (CTD) systems and various expendable bathythermograph systems (XBT), are registering SST in SST_{depth} layer. In all cases, these temperature observations are distinct from those obtained using remote sensing techniques and measurements at a given depth arguably should be referred to as 'sea temperature' (ST) qualified by a depth in meters rather than sea surface temperatures (Donlon *et al.*, 2002).

Figure 1 illustrates schematically the importance of referencing the mean depth or wavelength at which an SST measurement is determined, when it is considered upper-ocean SST. Figure 1(a) shows the characteristic thermal structure at night or during moderate to strong winds during the day that homogenize the temperature in the

upper-water layers. Figure 1(b) shows the characteristic situation for late morning–early afternoon following a period of light or absent wind and insulation. During the day, in clear sky, calm conditions, thermal stratification of the top few meters of the ocean will occur, resulting in significant temperature differences between SST_{int}, SST_{skin}, $SST_{subskin}$, and SST_{depth}. Under these conditions, surface temperature deviations greater than 3ºC, referenced to subsurface temperatures, are not uncommon and may persist for hours (Gentemann *et al.*, 2003). This underscores the motivation to refine the traditional reference to bulk SST, universally used in Oceanography and Meteorology, to the more exact parameter, SST_{depth}. Since SST retrievals by satellites are sensitive to a thin surface layer, the diurnal warming effect strongly influences these measurements (Gentemann *et al.*, 2003).

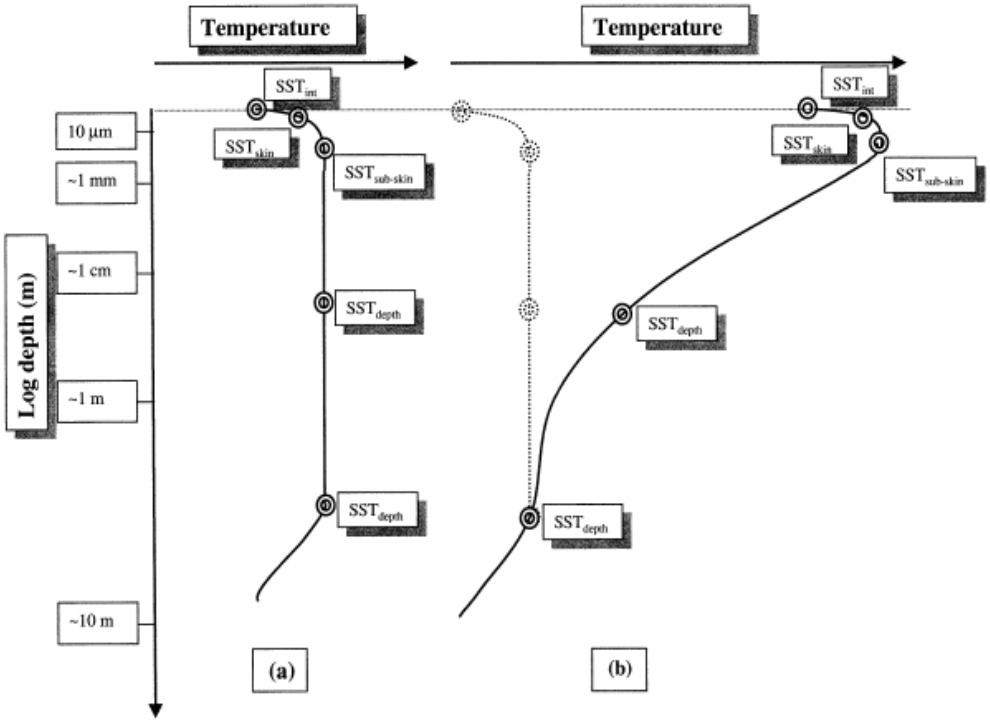

Figure 1 - Idealized temperature profiles of the near-surface layer (10-m depth) of the ocean during (a) nighttime and daytime with strong wind conditions and (b) daytime low–wind speed conditions and high insolation resulting in thermal stratification of the surface layers. (Adapted from Donlon *et al*. 2002)

The cloud-free conditions described by Fig. 1(b) are favorable for infrared remote sensing of SST from satellite instruments and in such cases, the significant vertical variation of SST demands careful attention in terms of SST data product conception, validation, and interpretation (Donlon *et al.*, 2002).

In this work we will use SST in the sense of skin sea-surface temperature measured from satellites.

2.3. Remote Sensing Measurements of SST

The integrity of all satellite-derived SST estimates is dependent of accurate instrument prelaunch characterization and post-launch self-calibration, and may also be limited by data processing procedures and local variations in air-sea interaction (Brown *et al*, 1993). However, the quality and credibility of derived data products depends on accounting comprehensively for the uncertainties associated with the measurement itself, the accuracy of atmospheric correction algorithm and, the changes within satellite sensors throughout their lifetime (Brown *et al*, 1993).

Since 1981, the NOAA series of polar-orbiting spacecraft have carried the Advanced Very High Resolution Radiometer (AVHRR), an instrument with three infrared (IR) channels suitable for estimating SST (Fox *et al.*, 2005). These channels are located in the wavelength regions between 3.5µm and 4µm and between 10µm and 12.5µm, where the atmosphere is comparatively transparent (Evans and Podestá, 1998). At IR wavelengths, the ocean surface emits radiation almost as a blackbody. In principle, without an absorbing and emitting atmosphere between the sea surface and the satellite, it would be possible to estimate SST using a single channel measurement. In reality, surface-leaving infrared radiance is attenuated by the atmosphere before it reaches a satellite sensor.

The fundamental measurement made by AVHRR sensors installed on NOAA's satellites is the upwelling radiance at the height of the satellite sensor specified for a number of spectral intervals and atmospheric path-length. For views of the sea surface, the calibrated radiance is composed of sea surface, direct atmospheric and reflected surface radiance; therefore, it is necessary to make corrections for atmospheric effects. Absorption and emission along the atmospheric path between the sea surface and satellite sensor (ignoring aerosol contributions) occurs, principally, due to water vapor, carbon dioxide, and ozone (Minnett, 1990). Among them, absorption due to water vapour accounts for most of the needed correction (Barton *et al.*, 1989). Another source of error is aerosol absorption. The aerosol content in the

atmosphere is increased during volcanic eruptions and large dust storms such as those from the Sahara. SST measurements are derived by compensating for unwanted radiance components reflected at the sea surface and the atmospheric attenuation of the emitted oceanic radiance. This is achieved using a weighted combination of spectral and view-specific radiant temperatures or ‘‘brightness temperatures’’.

The history of SST computation from AVHRR radiances is discussed at length by (McClain *et al.*, 1985), but, briefly, radiative transfer theory is used to correct for the effects of the atmosphere on the observations by utilizing "windows" of the electromagnetic spectrum where little or no atmospheric absorption occurs. Channel radiances are transformed (through the use of the Planck function) to units of temperature, and then compared to a-priori temperatures measured at the surface. This comparison yields coefficients which, when applied to the global AVHRR data, give estimates of surface temperature which have been nominally accurate to 0.3 ºC (Vazquez *et al.*, 1998).

2.4. Definition of Ocean Color

In the open ocean the most of colored matter near the ocean surface results from the presence and activities of microscopic organisms that make up the base of the marine food chain. Among these organisms, the phytoplankton alter the ocean optical properties most effectively - the absorption coefficient, the scattering coefficient, and the volume scattering function, - in a manner that gives rise to changes in color of the ocean surface. The phytoplankton also alters the effective penetration of visible light (Lewis, 1995).

Water containing phytoplankton has much more complex spectral characteristics, because the living cells of these small plant organisms typically contain colored pigments, as chlorophyll, used for photosynthesis. The reaction of photosynthesis uses solar power as its energy source, thus strongly absorbs sunlight in certain parts of the spectrum. Also detritus of dead organisms may contain skeletal material which contributes to light scattering and light-absorbing organic matter, even though the chlorophyll is no longer present in the dead cells. Consequently water containing

phytoplankton has different proportions of absorbing and scattering elements according to the species and the age of the population (Lewis, 1995).

The color of the ocean results from solar energy which is backscattered from the ocean surface and interior. The deep blue of the open oligotrophic waters results from the selective absorption and scattering of pure seawater, only slightly changed by phytoplankton or other optically active substances. As one moves closer to the shore, the consequent increase of concentration of phytoplankton changes the color from blue to green.

Pure ocean water is transparent to blue and green wavelengths, but is strongly absorbing at longer wavelengths. Different absorption spectra are typical for Chromophoric Dissolved Organic Matter (CDOM) and phytoplankton pigments, such as chlorophyll *a*. Chlorophyll *a*, the most abundant photosynthetic pigment found in phytoplankton, has a primary absorption peak near 440 nm. CDOM absorption monotonically increases as wavelength decreases into the ultraviolet (UV). At the same time, scattering from water particles enhances reflectance at longer wavelengths. The net result is a shift from blue water to brownish water as pigment and particulate concentrations increase (McClain, 2008). The questions are whether or not changes in the spectral reflectance are sufficiently correlated with a single pigment concentration such as chlorophyll *a* to be quantitatively useful and, if that's the case, whether or not accurate observations of ocean reflectance could be made from a satellite so that large areas could be surveyed rapidly and routinely.

2.5. Remote Sensing Measurements of Ocean Color

One of the first remote sensing demonstrations that the shift in spectral shape related to chlorophyll *a* concentration can be instrumentally registered was done with airborne sensor to measure the spectra of backscattered light from the sea (Clarke *et al.*, 1970).

Still atmospheric contribution to the total reflectance, measured by an ocean color sensor, increases dramatically with altitude as a result of Rayleigh (gas molecules) and aerosol scattering. In fact, at the top of the atmosphere, the radiance emanating out of the water column contributes no more than 15% of the total outgoing radiance

(McClain, 2008). To remove the effect of atmosphere, a correction scheme needs to accurately account for numerous scattering (gases and aerosols), absorption (at least ozone absorption), and surface reflection (sun glint) effects, for a wide range of solar and sensor-viewing geometries (McClain, 2008). In 1978 NASA launched Nimbus-7 satellite carrying the first scanning radiometer, operating in visible and near-visible wavelengths and primarily designed to observe ocean color, known as the Coastal Zone Color Scanner (CZCS) (Robinson, 1985). The CZCS had ocean color bands at 443, 520, and 550 nm for quantifying changes in the marine spectral slope with pigment concentration (McClain, 2008).

After the CZCS (1978–1986) demonstrated that quantitative estimations of geophysical variables such as chlorophyll *a* and diffuse attenuation coefficient could be derived from the radiances, registered at the top of the atmosphere, a number of international missions with ocean color sensors were launched, beginning in the late 1990s. The most known examples are: the Ocean Color and Temperature Sensor (OCTS, Japan, 1996–1997), the Sea-viewing Wide Field-of-view Sensor (SeaWiFS, United States, 1997-present), two Moderate Resolution Imaging Spectroradiometers (MODIS, United States, Terra/2000-present and Aqua/2002-present), the Global Imager (GLI, Japan, 2002–2003), and the Medium Resolution Imaging Spectrometer (MERIS, European Space Agency, 2002-present). These missions have provided data of exceptional quality and continuity, allowing to cover a wide variety of marine research topics (McClain, 2008).

In this investigation MODIS sensor is used to retrieve normalized water-leaving reflectance necessary to estimate chlorophyll *a* concentration. The Moderate Resolution Imaging Spectroradiometer (MODIS), a major NASA Earth observing System (EOS) instrument, was launched aboard the Terra satellite on December 18, 1999 (10:30 AM equator crossing time, descending) for global monitoring of the atmosphere, terrestrial ecosystems, and oceans. On May 4, 2002, a similar instrument was launched on the EOS-Aqua satellite (1:30 PM equator crossing time, ascending). The EOS Project is designed to collect data for 15 years in order to differentiate short-term and long-term trends, as well as, regional and global phenomena. MODIS, with its 2330 km viewing swath width flying onboard Terra and Aqua, provides almost complete global coverage in one day. It acquires data in 36 high spectral resolution

bands between 0.415 and 14.235 nm with spatial resolutions of 250 m (2 bands), 500 m (5 bands), and 1000 m (29 bands) (Savtchenko *et al.*, 2004). Ocean color sensors like MODIS, have been used extensively in oceanographic studies to quantify the processes responsible for the observed phytoplankton patterns. The radiance measured by MODIS at high spatial resolution provides improved and valuable information about the physical structure of the Earth's atmosphere and surface (Barnes *et al.*, 1998), and provides a long term data set with the same geophysical parameters for the study of climate and global change studies (Salomonson *et al.*, 2001, Savtchenko *et al.*, 2004).

3. DATA SETS AND METHODS

3.1. AVHRR Data

This study uses the Sea Surface Temperature (SST) satellite images obtained from NOAA (16 and 17) Advanced Very High Resolution Radiometer (AVHRR) to study spatial and temporal variability of SST in the NE Subtropical Atlantic. The initial images were processed at University of Miami's Rosenstiel School of Marine and Atmospheric Science (RSMAS) in partnership with the NOAA National Oceanographic Data Center (NODC)[1]. NOAA/AVHRR derived SST values (in ºC) were obtained using the Multi-Channel SST (MCSST) algorithm (McClain *et al*., 1985) and then averaged to 9-day temporal resolution and 4 km spatial resolution. In this investigation we used monthly means for the period January 2002 to December 2006 (a total range of sixty months), processed by the Physical Oceanography Distributed Active Archive Center (PO.DAAC) at the Jet Propulsion Laboratory (JPL) of the California Institute of Technology and the National Aeronautics and Space Administration (NASA). The data are available at PO.DAAC (2008).

To avoid the diurnal thermocline formation effect and minimize the difference between surface skin layer and mixed layer temperature, only night time images were used. The resulting images contained remnant errors. To improve atmospheric noise removal the images were post-processed with a threshold filter, e.g. the SST values less than 10ºC in the northern part of the region and for upwelling zones, and less than 12ºC for the central and southern parts of the region, were excluded from further analyses. The threshold values for the region were chosen based on conclusions of Lafon *et al*. (2004).

1. For further details about AVHRR SST data processing, validation and technical specifications please visit:

- http://podaac.jpl.nasa.gov/DATA_CATALOG/avhrrinfo.html
- http://www.rsmas.miami.edu/groups/rrsl/pathfinder/Matchups/match_index.html ;

3.2. MODIS DATA

Ocean Color (OC) images were obtained from the Moderate Resolution Imaging Spectroradiometer (MODIS) installed on AQUA satellite. The initial images were processed by the Ocean Data Processing System (ODPS) at NASA's Goddard Space Flight Center[2]. Chlorophyll *a* concentrations (in mg/m^3), were obtained using the Case 1 Chlorophyll *a* algorithm (Carder *et al*., 2003), and then averaged to 9-day temporal resolution and 4 km spatial resolution. For this study we used monthly means for the period of July 2002 to December 2007 (the total range of fifty four months) available from the "Ocean Color Level 3 browser" (OceanColor Web, 2008).

To improve atmospheric noise removal the images were post-processed with a threshold filter. Values higher than 7 mg/ m^3 and 20 mg/ m^3 were excluded from further analyses in oceanic and upwelling zones, respectively. Threshold values of chlorophyll *a* for the region were chosen based on the work by Martins *et al*. (2007)

3.3. Definition of Regions

The area for this study is defined as a 15 ºx29º latitude–longitude box extending from 30ºN to 45ºN and from 6º W to 35º W. To ensure that zones with distinct water characteristics were covered, as well as, for further statistical analyses, nine sub-regions, distributed over the whole area, were defined (Figure 2 and Table 1).

[2]. For further details about MODIS OC data processing, validation and technical specifications please visit:

- http://oceancolor.gsfc.nasa.gov/DOCS/MODISA_processing.html ;

- http://oceancolor.gsfc.nasa.gov/VALIDATION/ ;

- http://oceancolor.gsfc.nasa.gov/DOCS/;

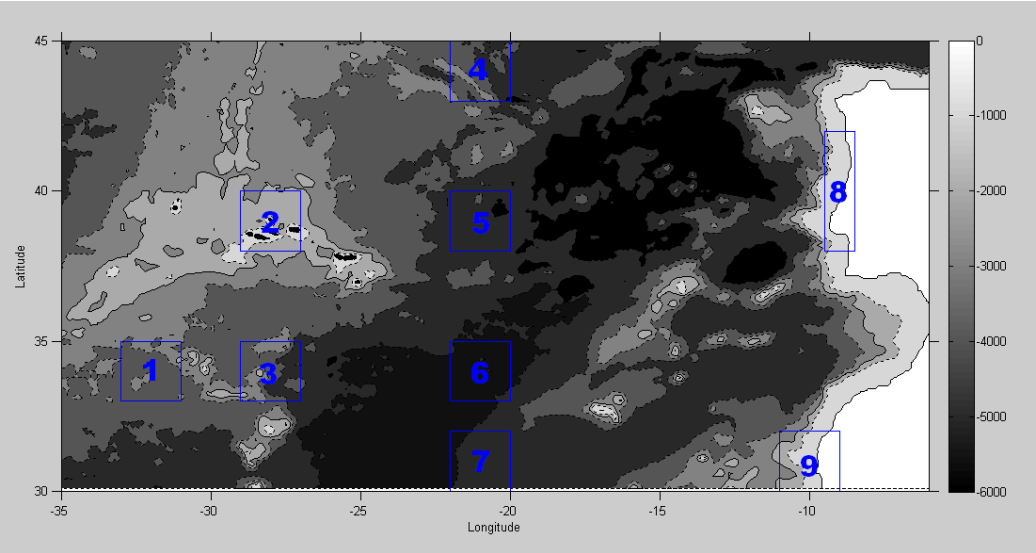

Figure 2 – **Map of general bathymetry (m) of the region of study and selected sub-regions.**

Table 1 - **Geographic limits and number of pixels in each of the selected sub-regions.**

Square	Latitude range	Longitude range	No. of Pixels
1	33ºN – 35ºN	33ºW – 31ºW	2163
2	38ºN – 40ºN	29ºW – 27ºW	2128
3	33ºN – 35ºN	29ºW – 27ºW	2163
4	43ºN – 45ºN	22ºW – 20ºW	2163
5	38ºN – 40ºN	22ºW – 20ºW	2163
6	33ºN – 35ºN	22ºW – 20ºW	2163
7	30ºN – 32ºN	22ºW – 20ºW	2163
8	38ºN – 42ºN	9.5ºW - 8.5ºW	1362
9	30ºN – 32ºN	11ºW – 9ºW	1483

3.4. Temporal Scales

In this investigation, we based our results primarily on monthly and annual means. In some cases, when seasonal means were obtained, the seasons were distinctly defined for SST and OC. For SST, spring encompassed the months of April-June, summer – July-September, autumn – October-December, winter – January-March.

For OC, spring encompassed the months of March-May, summer – June-August, autumn – September-November, winter – December-February.

The reason for this seasonal choice difference results from the fact that previous works for the region show a *decalage* of about one month from initiation of surface

ocean warming and phytoplankton (expressed as satellite-derived concentration of near-surface Chl *a*) bloom triggering (e.g. Martins *et al.,* 2007).

3.5. Statistic Analysis

For all study areas and for both SST and OC, statistical parameters like monthly and annual averages, medians, and standard deviations were calculated from the monthly images. When we needed to eliminate the seasonal cycle, monthly anomalies (ΔSST and ΔOC) were calculated using the following formulas:

ΔSST = (Monthly SST median) - (inter-annual average of monthly SST median);

ΔOC = (Monthly OC median) - (inter-annual average of monthly OC median).

Resulting monthly anomaly values were cross-correlated to get statistical dependence between the parameters. Annual mean anomalies were also correlated with the annual mean North Atlantic Oscillation (NAO) index. The corresponding annual mean NAO indexes were calculated based on monthly mean NAO index values obtained from the Climate Prediction Center (CPC) at NOAA's National Center for Environmental Prediction (NCEP) web site (Climate Prediction Center, 2008)[3].

[3] For further details about monthly NAO indexes calculation please visit:
- http://www.cpc.ncep.noaa.gov/products/precip/CWlink/pna/nao.shtml ;

4. RESULTS

4.1. Patterns Analysis

4.1.1. Analysis of SST Patterns

4.1.1.1. General Mean

Distribution of the SST field for the years 2002 to 2006 was obtained from annual means PO.DAAC's AVHRR Pathfinder SST v5 data by taking the median values in each pixel-point of the image (Figure 3). The highest intra-annual median SST values are observed south of 35^{o}N, in the south-western corner of the image, where they reach 22-23ºC. The lowest SST values are characteristic at the north-eastern part of the region and the coast of Iberian Peninsula (14-17 °C). The median SST over the Azores region is in the range of 18-21°C.

Figure 3 also shows a strong latitudinal SST gradient with the median surface temperature increasing towards south, or more precisely to the south-south-west. A longitudinal SST gradient is also present. The zonal isotherm tilt possibly reflects an effect of advection patterns on the SST, forcing the isotherms to deviate from the zonal position.

At the western coast of the Iberian Peninsula SST medians are significantly lower than in the surrounding waters, with values ranging between 14ºC and 15ºC in the northern part and 16-17ºC to the south. This is a result of coastal upwelling, characteristic for the region (Matzen, 2004). Similar processes occur on the West African coast, where the mean surface temperature is in the range of 16-19ºC.

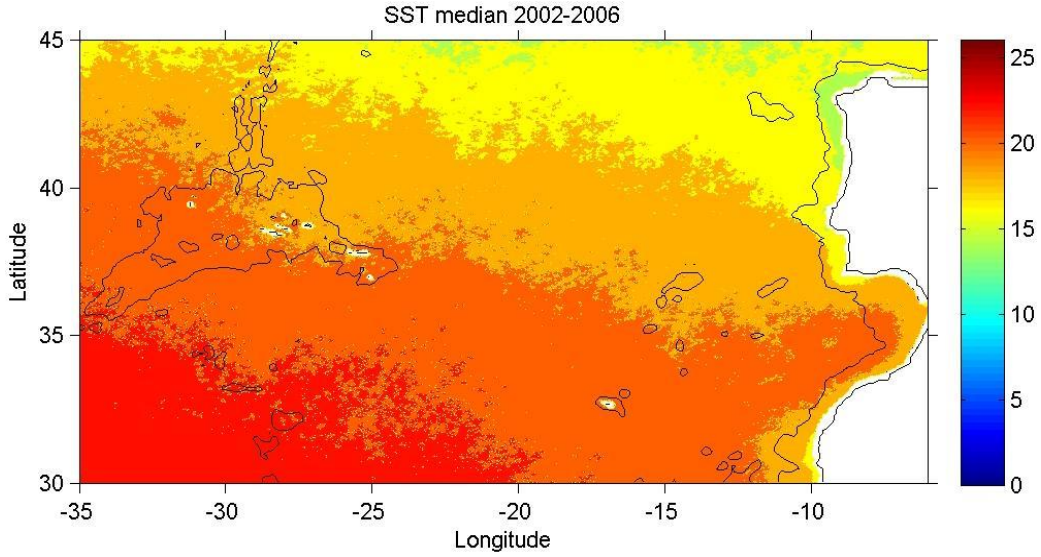

Figure 3 - General median distribution of SST for the years 2002 to 2006 obtained from the PO.DAAC's AVHRR Pathfinder SST v5[4]

The black contour represents the 2000 m depth, delineating approximately the region of the Mid Atlantic Ridge (MAR). The Azores and Madeira islands, mainland Portugal, Spain and Africa are marked in white.

4.1.1.2. Seasonal Variability

The mean seasonal variation of the SST field for the years 2002 to 2006 was obtained from PO.DAAC's AVHRR Pathfinder SST v5 monthly mean images (Figure 4). Months range for each season is: January-March (winter), April-June (spring), July-September (summer) and October-December (autumn).

As expected, seasonal warming of the waters is clearly evident with isotherm advancing during spring and summer and retreating during autumn and winter. The most northern region (square 4) presents mean values ranging between 12°C (winter) and 18°C (summer), while the most southern region (square 7) presents values ranging between 18ºC (winter) and 24ºC (summer).

Isotherm tilt is clearly evident during summer with a warm water entrance from the southwest. For instance, squares 1 and 3, although located at the same latitude, are inside the 24 ºC zone, while SST at square 6 is 1-2 ºC colder. In winter isotherm tilt also occurs, with for instance Azores region (square 2) between the 14-16ºC isotherms and square 5, located at the same latitude, inside the 14ºC zone.

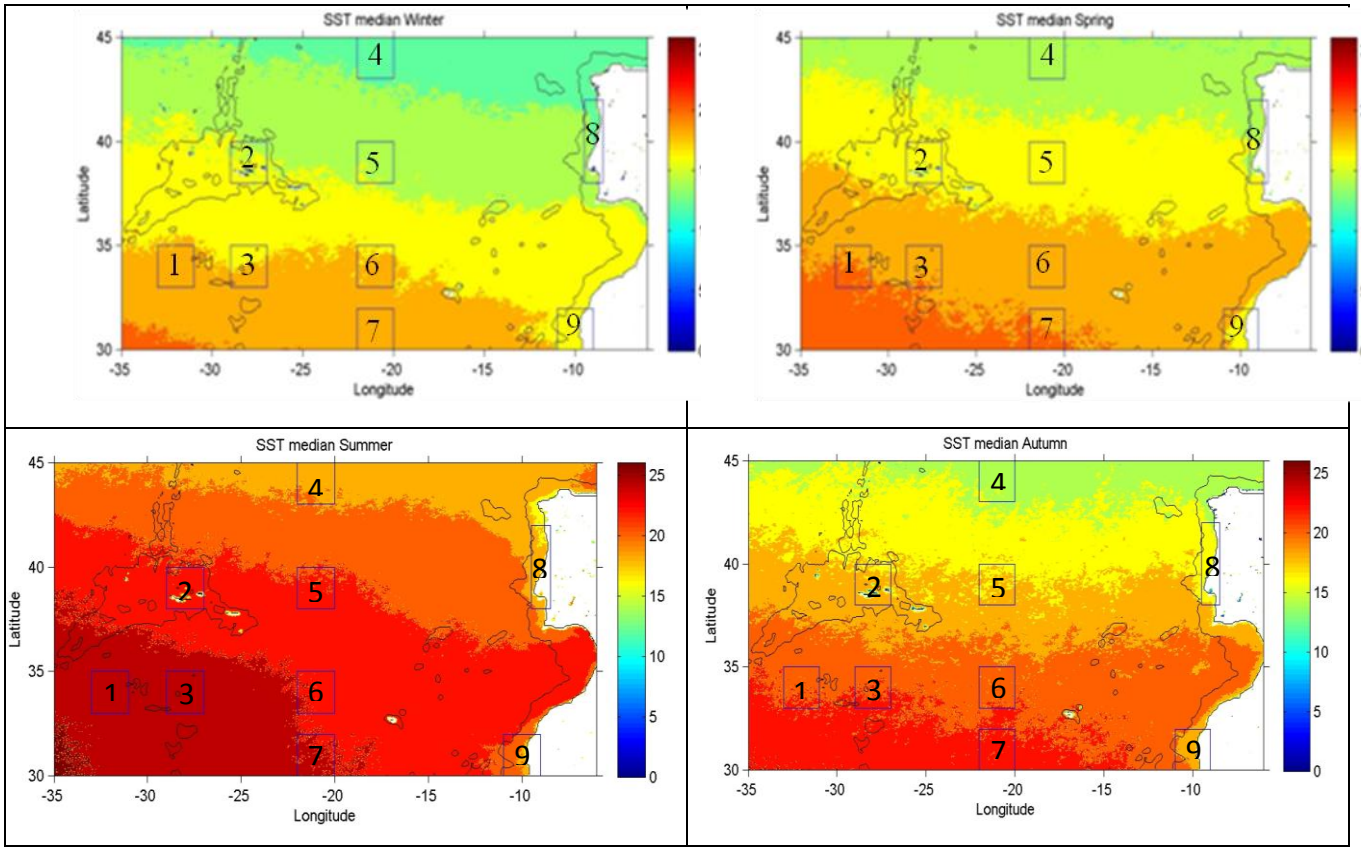

Figure 4 - Seasonal mean distribution of SST for the years 2002 to 2006 obtained from PO.DAAC's AVHRR Pathfinder SST v5. The black contour represents the 2000 m depth, delineating approximately the region of the Mid Atlantic Ridge (MAR). The Azores and Madeira islands, mainland Portugal, Spain and Africa are marked in white. The blue contoured squares represent the selected regions of study (see chapter 3).

4.1.1.3. Inter-Annual Variability

The annual mean SST fields for the years 2002 to 2006 were obtained in each point as the medians values of the monthly mean, obtained from PO.DAAC's AVHRR Pathfinder SST v5 data (Figure 5). A strong latitudinal gradient and general NW/SE tilt of isotherms is visible for all years.

Year 2004 was the warmest with a mean temperature in the Azores region (square 2) of 18ºC and with the 14ºC isotherm reaching the 45ºN over MAR. In contrast, the year 2002 is clearly the coldest one with a mean temperature at 45ºN falling below 12ºC and the temperature over the Azores plateau (square 2) being below 16ºC.

Longitudinal annual mean gradients also change from year to year. Thus, in 2006 the isotherms stayed more or less horizontal. In 2002, oppositely, the isotherm tilt was quite high. This year the 20ºC annual mean isotherm did not reach the 15ºW. In 2004

warm water with a mean temperature of 22ºC extended until 20ºW zone, but north of 35°N the tilt was probably the highest.

Inter-annual variability in coastal regions (squares 8 and 9) is also evident (cf. Figure 2). In 2005 and specially 2006 there was a clear temperature increase in these regions. In 2006, probably due to the absence of isotherms tilt, water with mean temperatures of 18-19ºC reaches the 40ºN in the western coast of Portugal. Minimum SST in these regions was registered during 2002 with a mean temperature of 14-15ºC in the coast of Portugal and 16-17ºC in the West African coast.

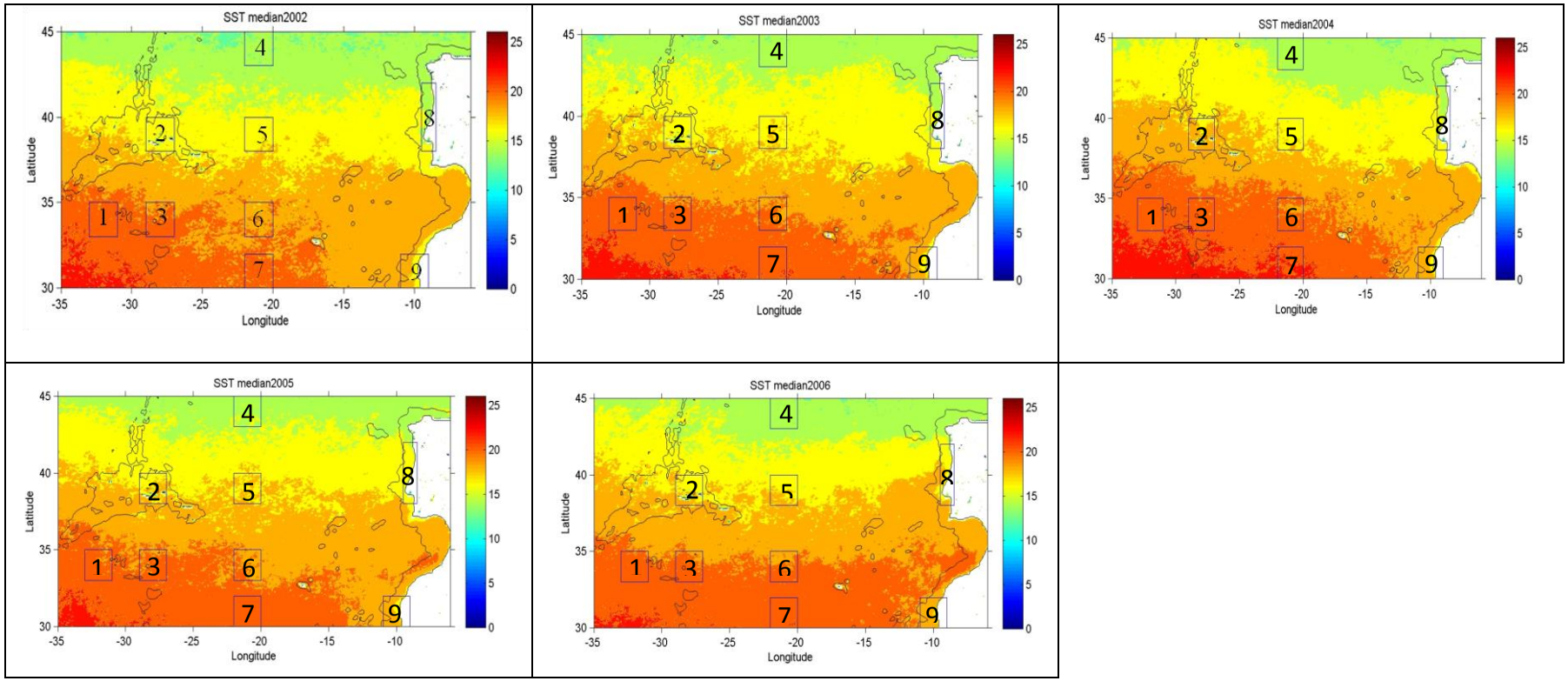

Figure 5 - Annual mean distribution of SST for the years 2002 to 2006 obtained from PO.DAAC's AVHRR Pathfinder SST v5. The black contour represents the 2000 m depth, delineating approximately the region of the Mid Atlantic Ridge (MAR), the Azores and Madeira islands, mainland Portugal, Spain and Africa. These regions are marked in white. The blue contoured squares represent the selected regions of study (see chapter 3).

4.1.2. Analysis of Ocean Color Patterns

4.1.2.1. General Mean

Distribution of the OC field for the years 2002 to 2006 was obtained from NASA's MODIS chlorophyll annual means data by taking the median values in each pixel-point of the image (Figure 6). The highest intra-annual median chlorophyll *a* values are observed in the west coast of Portugal and Africa where values are superior to 0.5 mg/m^3.In the Northeast part of the region, they reach 0.4-0.5 mg/m^3. The lowest OC values are characteristic at the south-western part of the region (<0.1 mg/m^3). The median chlorophyll over the Azores region is in the range of 0.15-0.2 mg/m^3 with slightly increased concentration near the coast of the islands.

Figure 6 also shows a general latitudinal OC gradient with median chlorophyll increasing towards north, or more precisely to the northeast. A slight longitudinal OC gradient is present with higher chlorophyll concentration in the eastern part.

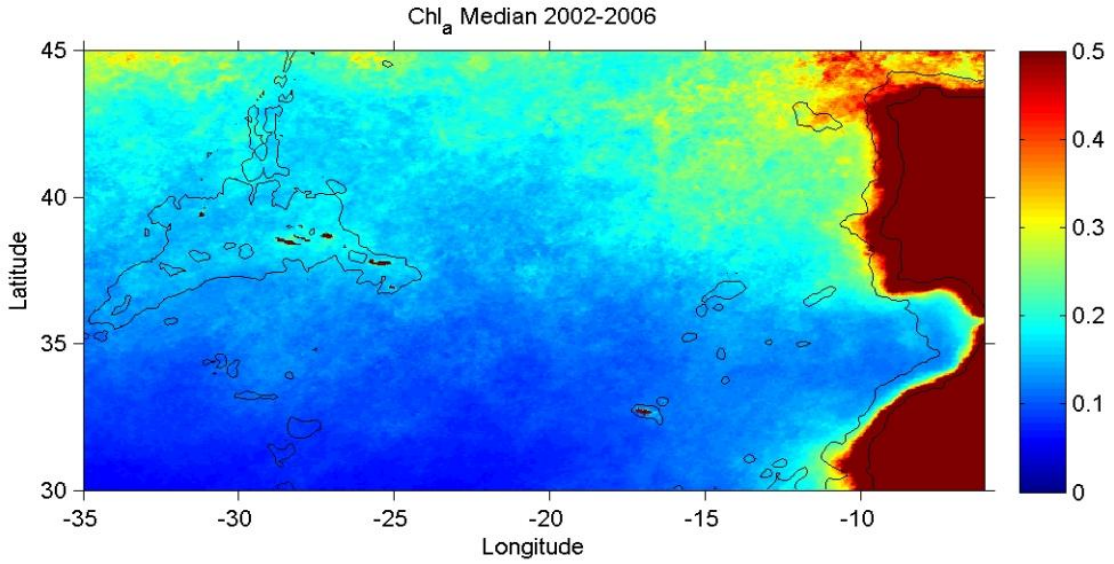

Figure 6 - General median distribution of OC for the years 2002 to 2006 obtained from the Ocean Color Level 3 browser[1]. The black contour represents the 2000 m depth, delineating approximately the region of the Mid Atlantic Ridge (MAR). The Azores and Madeira islands, mainland Portugal, Spain and Africa are marked in red.

[1] http://oceancolor.gsfc.nasa.gov/cgi/l3;

4.1.2.2. Seasonal Variability

The mean seasonal variation of the OC field for the years 2002 to 2006 was obtained from NASA's MODIS chlorophyll monthly mean images (Figure 7). Months range for each season is: December-February (winter), March-May (spring), June-August (summer) and September-November (autumn).

Strong OC seasonal patterns are evident in all regions, with highest chlorophyll *a* concentration during springtime and lowest in summer. During spring, strong blooms (>0.5 mg/m^3) occur in the northeast part of the region. In latitudes between 36-41ºN small winter blooms occur (0.2-0.3 mg/m^3), mainly in the Azores area. During summer and autumn, stratification of the upper layer is high and so small blooms only occur on the northern part of the region.

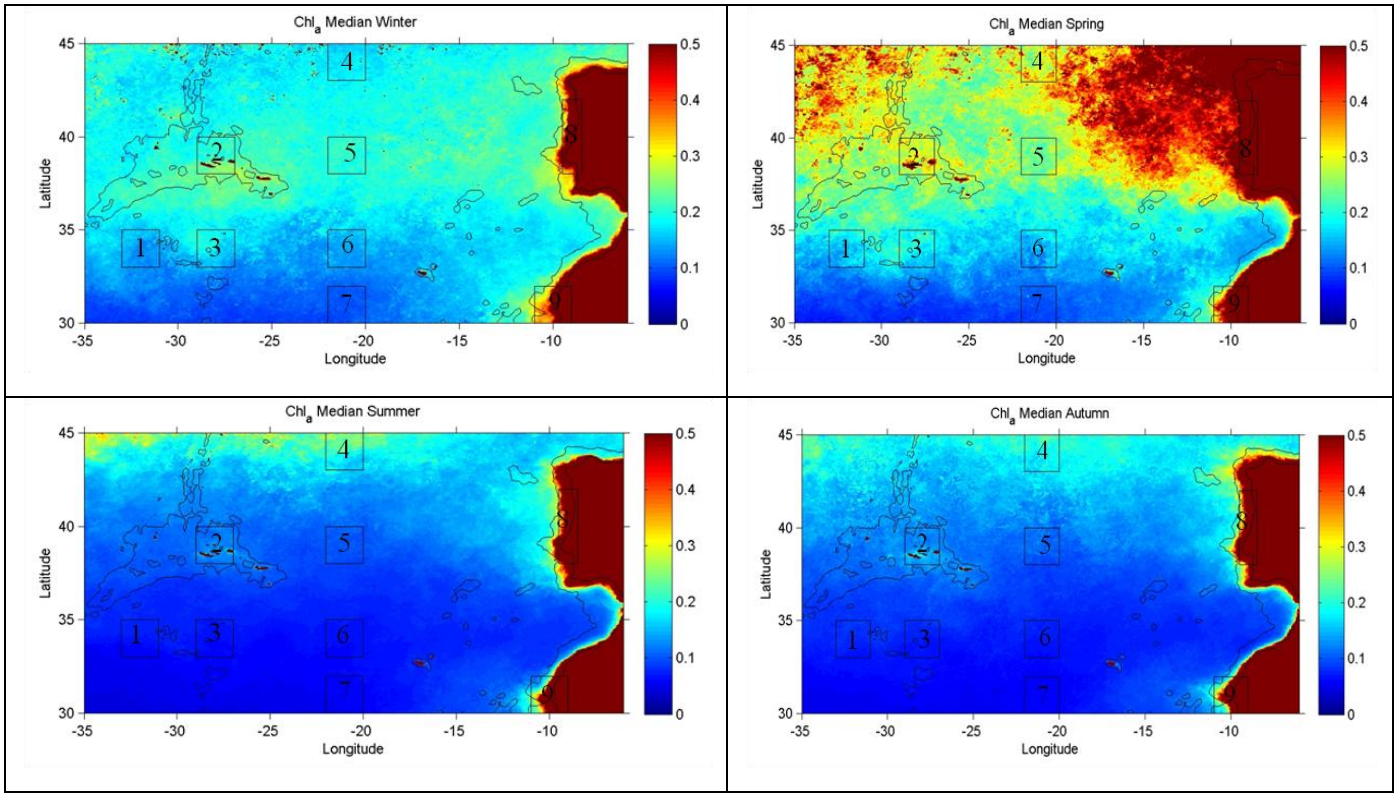

Figure 7 - Seasonal mean distribution of OC for the years 2002 to 2006 obtained from Ocean Color Level 3 browser. The black contour represents the 2000 m depth, delineating approximately the region of the Mid Atlantic Ridge (MAR). The Azores and Madeira islands, mainland Portugal, Spain and Africa are marked in red. The black contoured squares represent the selected regions of study (see chapter 3).

4.1.2.3. Inter-Annual Variability

The annual mean OC fields for the years 2002 to 2006 were obtained in each point as the medians values of the monthly mean, obtained from NASA's MODIS chlorophyll monthly mean images (Figure 8).

Distinct OC patterns are evident in the 5 years. All years show a general tendency for chlorophyll concentration to increase towards northern regions. In 2005 and 2006 some increased chlorophyll values are present in southern latitudes, contrasting with year 2002 that generally presents very low values in the whole study area. During 2003 strong blooms (>0.5 mg/m^3) occurred in the most northern region (square 4). In 2004 and 2005 the strongest blooms appear on the north coast of the Peninsula Iberian, while in 2005 the highest values were found in the northeast part of the region, west of Portugal. Annual variability is also evident in the Portuguese coast region (square 8) where increased chlorophyll values are found in 2005 and 2006.

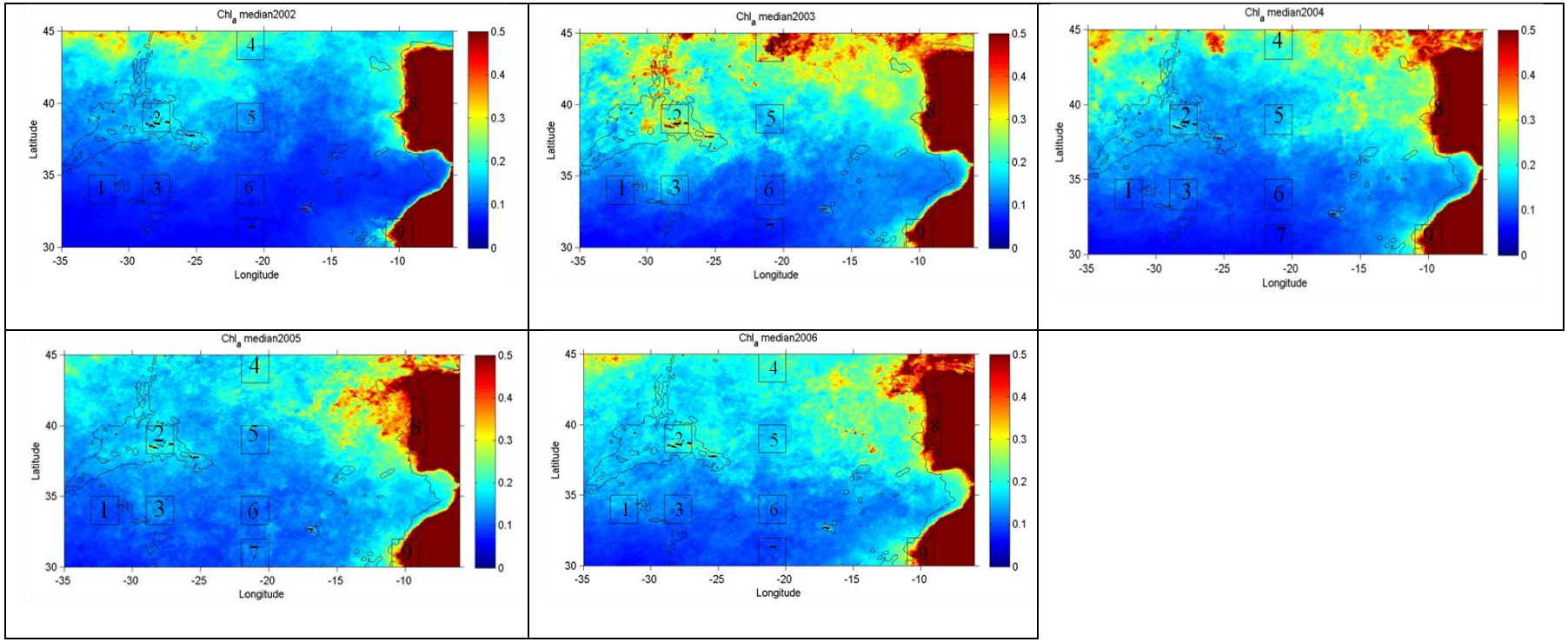

Figure 8 - Annual mean distribution of OC for the years 2002 to 2006 obtained from Ocean Color Level 3 browser. The black contour represents the 2000 m depth, delineating approximately the region of the Mid Atlantic Ridge (MAR). The Azores and Madeira islands, mainland Portugal, Spain and Africa are marked in red. The black contoured squares represent the selected regions of study (see chapter 3).

4.2. Statistics for selected regions

4.2.1. Temporal Variability of SST

4.2.1.1. Seasonal Variability

SST inter-annual monthly means derived from AVHRR imagery show similar seasonal cycle among all oceanic regions (Figure 9). Seasonal warming and cooling of the waters is clearly evident, with mean temperature rising during spring and summer and falling during autumn and winter. August is the month where all regions reach a maximum temperature value, with an exception for the most southern region (square 7), where SST reaches its maximum only in September. The amplitudes between winter SST minimum and summer SST maximum in all regions are around 6-7ºC.

In coastal regions (square 8 and 9), the inter-annual monthly mean SST curve (Figure 10) shows somewhat distinct pattern. The mean temperature rises during early spring and maintains more or less stable values during summer time. In contrast with oceanic regions typical maximum during August is not that clearly pronounced in coastal regions. The seasonal temperature amplitudes in these regions are also lower, of the order of 4-5ºC.

The last two Figures (9 and 10) show the highest surface temperatures during summertime in square 1 (25.4ºC) and the lowest during winter in square 4 (13.4ºC). A latitudinal effect seems clearly the main source for the differences observed between SST seasonal cycles in the region. Normally, higher latitudes are characterized by lower surface temperatures throughout a year. Another important factor, regulating the height and the shape of seasonal cycles, is the difference between the mean longitudes of the areas. Figure 9 shows a comparison between regions located at the same latitude, but at different longitudes. On the graphic it is possible to see a clear decrease in temperature as we move eastwards (from squares 1 $\rightarrow$ 3 $\rightarrow$6). This last region (square 6) also presents the lowest inter-annual temperature amplitud

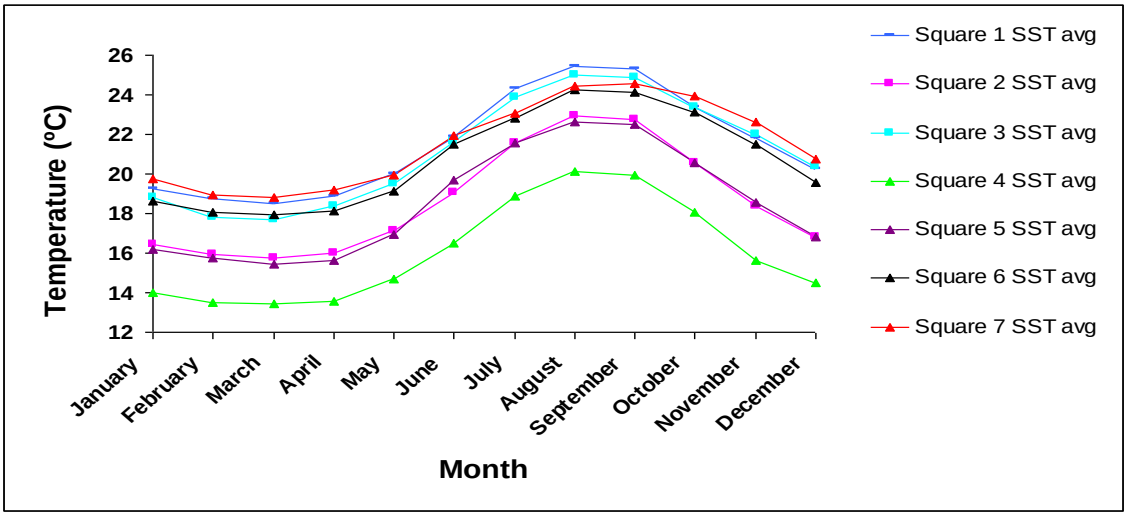

Figure 9 - AVHRR SST all monthly means from 2002 to 2006 for oceanic regions.

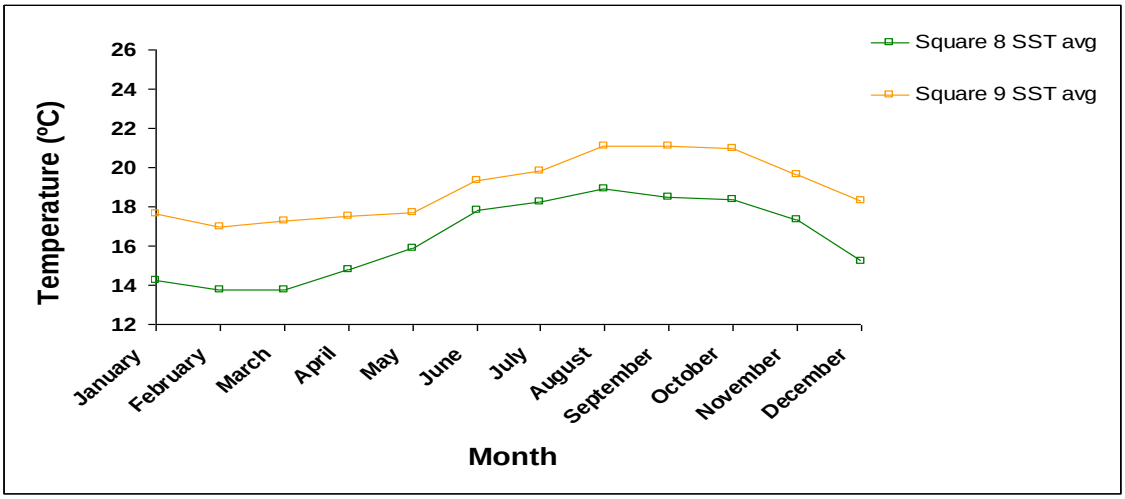

Figure 10 - AVHRR SST all monthly means from 2002 to 2006 for coastal regions.

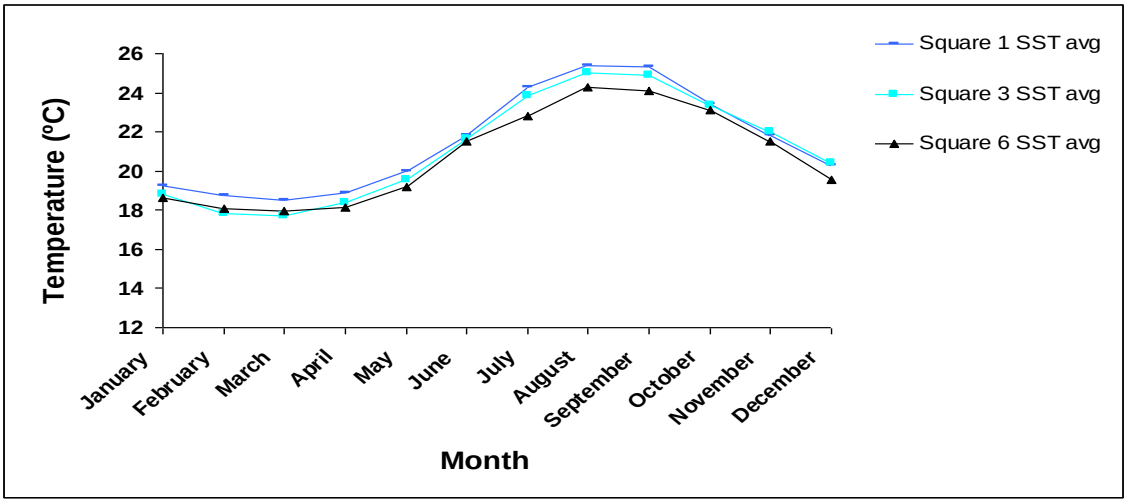

Figure 11 - AVHRR SST all monthly means from 2002 to 2006 for squares 1, 3 and 6.

4.2.1.2. Inter-annual Variability

Monthly median SST values derived from AVHRR imagery are presented in Figure 12. IN general, a clear seasonal warming during spring and cooling during autumn is characteristic for all the years for all the regions in study. Nevertheless, the graphic shows distinct seasonal cycles between years with, for instance, a clear different pattern in 2004 where more northern regions (squares 2, 4 and 5) present lower and more stable SST values during summer and higher and more stable SST minimum during winter. Also in 2004, the southern regions (squares 1, 3, 6 and 7) show better SST agreement among them, than on other years. In fact, particularly during summer, these four stations mean surface temperatures are about 2°C higher than all other regions for the same year. In Figure 12 is also possible to see that coastal regions (squares 8 and 9), show a distinct pattern when compared with oceanic regions.

Inter-annual comparison among different regions shows square 1 as the region with the highest SST maximum and highest SST values in summer, with the exception of year 2003 where square 3 gets the higher value. Northern regions tend to reach maximum SST values sooner than southern ones. During some years the time lag is about one month. Generally, the northern regions reach their maximum in August and southern regions in August-September. On the other hand, there is no clear tendency for minimum SST monthly median values. Square 4 presents the lowest SST in all years with exception of year 2005 where square 8 gets the lowest SST minimum.

Comparison of SST seasonal amplitudes for the same period shows that during the years 2003 (2004) the highest (lowest) SST amplitude in all regions was reached, with few exceptions, respectively. These are for example, square 4 that reached its maximum amplitude in 2005, and the coastal regions (squares 8 and 9) that do not have any significant inter-annual difference in amplitude.

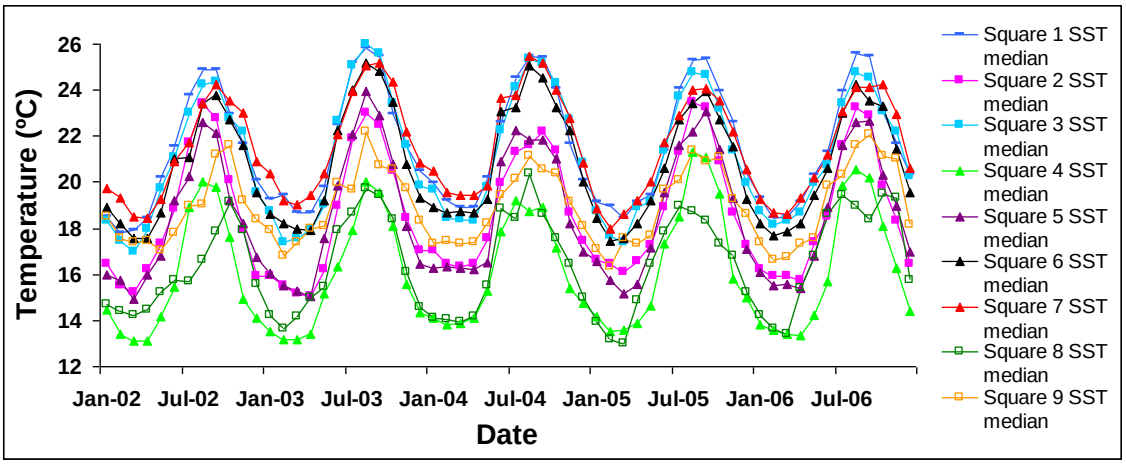

Figure 12 - AVHRR SST monthly medians from January 2002 until December 2006 for all regions.

4.2.2. Temporal Variability of Ocean Color

4.2.2.1. Seasonal Variability

Ocean Color all monthly means derived from MODIS imagery show different seasonal cycles for different oceanic regions (Figure 13).

Spring phytoplankton bloom is present in all regions with chlorophyll *a* concentration increasing during winter and early spring, and decreasing during late spring and summer. Results also show a small increase in chlorophyll *a* concentration during autumn in square 2 and mostly in square 4.

Mean chlorophyll *a* values over the year, are generally highest in the coastal regions of this study than in the oceanic ones. At the coast of Portugal (square 8), the inter-annual monthly mean OC curve (Figure 14) shows a completely distinct pattern, with chlorophyll *a* concentration increasing sharply during late winter reaching its maximum in early spring (March). Then chlorophyll *a* decreases, but another pronounced bloom occurs in summer, with mean concentration values reaching 0.99 mg/m^3 by August. The minimum value is obtained during late autumn (November). Results also show that the West African coastal region (Square 9) has no clear defined seasonal cycle. Here chlorophyll *a* concentrations values stay more or less stable with small variations over the year, though they tend to increase in spring.

Inter-annual monthly means (Figure 13 and Figure 14) also show the highest chlorophyll *a* values during springtime in square 8 (1.04 mg/m^3) and lowest during autumn in square 7(0.05 mg/m^3).

As latitude increases, regions (squares 2, 4 and 5) have more pronounced spring blooms and reach maximum chlorophyll *a* later in spring (May) contrasting with southern regions early spring blooms (March).

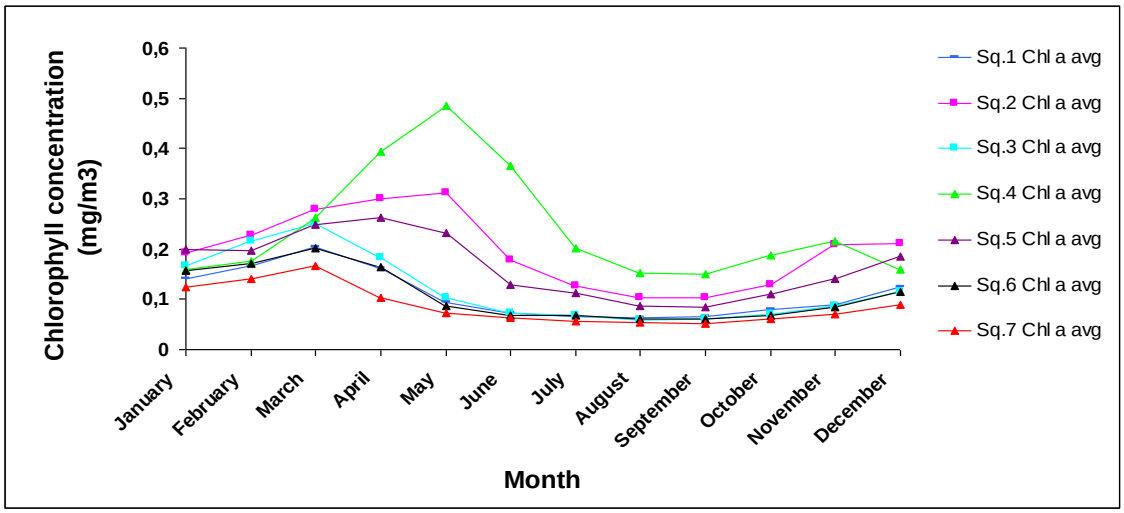

Figure 13 - MODIS OC all monthly means from 2002 to 2006 for oceanic regions.

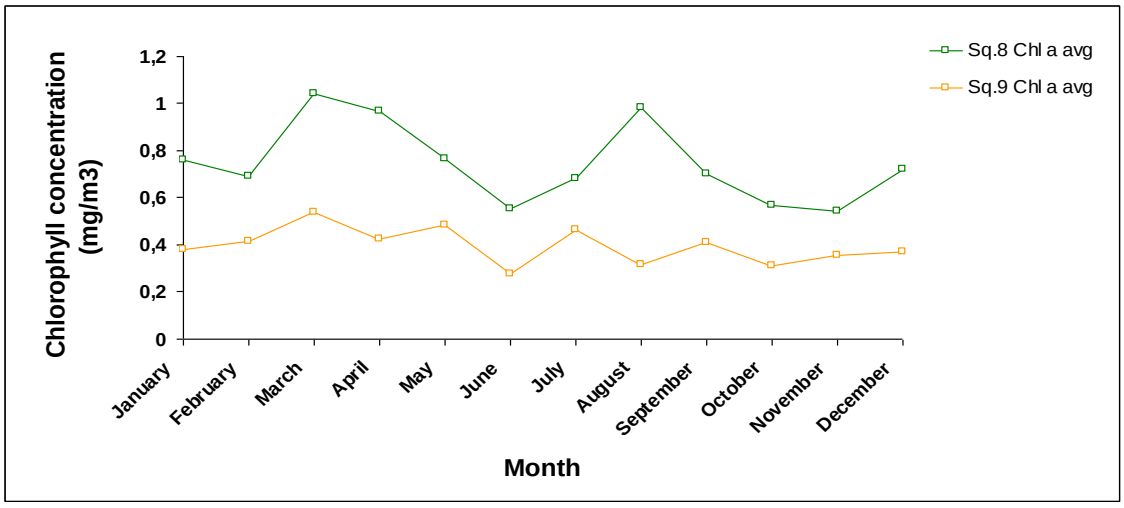

Figure 14 - MODIS OC all monthly means from 2002 to 2006 for coastal regions.

4.2.2.2. Inter-Annual Variability

Monthly mean OC values derived from MODIS imagery (Figure 15) show distinct seasonal cycles with increase (decrease) of Chl *a* pigments during February-May (August-September). In general, results for oceanic regions show highest values in square 4 particularly during May 2003 and June 2006. The year 2004 is an exception, with highest Chl *a* values in square 5. From Figure 15 it is also possible to see a clear tendency for the northern regions (squares 2, 4 and 5) to reach maximum chlorophyll concentration 1 or 2 months later than the southern regions (squares 1, 3, 6 and 7).

For coastal regions (squares 8 and 9), Figure 16 shows no clear chlorophyll *a* pattern over the year. During 2004 the chlorophyll values at square 8 were low. Mean chlorophyll *a* values in these regions are generally higher than in the open ocean regions. This is particularly true for the coast of Portugal (square 8) where the highest chl *a* value of 1.6 mg/m^3 occurs in March 2003. At the same time, the minimum values in all regions can reach 0.04 mg/m^3 (September 2003 and September 2004). Corresponding minimum value was observed only in the most southern oceanic region (square 7).

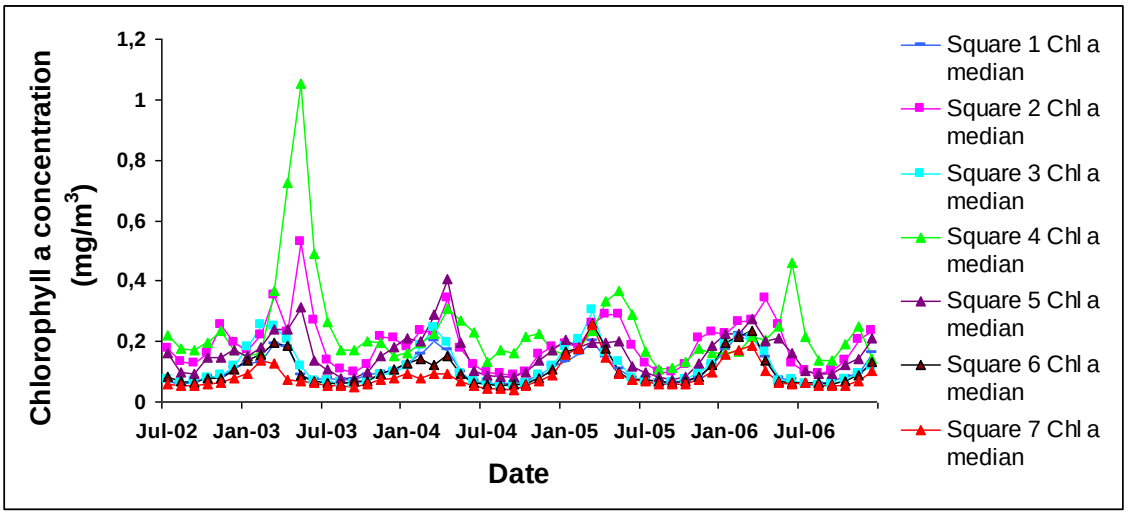

Figure 15 - MODIS OC monthly medians from July 2002 until December 2006 for oceanic regions.

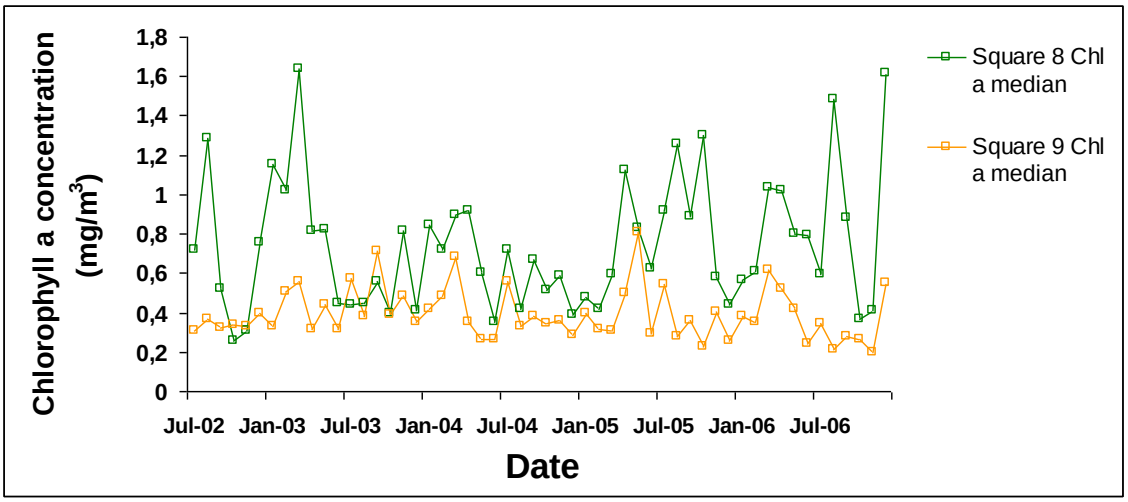

Figure 16 - MODIS OC monthly medians from July 2002 until December 2006 for coastal regions.

4.2.3. Variability of SST vs Ocean Color

4.2.3.1. Seasonal Variability

Monthly mean chlorophyll a concentrations, at seasonal time scale, show evident general tendency to behave inversely to SST. Table 2 shows the correlation coefficients (K) between SST and OC inter-annual monthly mean values from 2002 to 2006, for the selected regions. Significant correlation coefficients (at 1% level of significance) were found in all regions with exception for the most northern one (square 4) and coastal zones (squares 8 and 9). As an illustration, Figure 17 shows the inter-annual seasonal cycle of surface temperature and chlorophyll for square 5, where the most negative correlations were obtained. Except the short period of the spring bloom, the curves have clear inverse seasonal cycle. Figure 18 represents SST and chlorophyll behaviour for the most northern region (square 4) with the least correlation between the 2 parameters. Here there is no correspondence between the curves until May and then an inverse behaviour is observed on forward months.

Correlation coefficients between the inter-annual monthly means of SST and OC for the spring period (March to May) were also calculated, and the results are shown in Table 3. Despite correlations coefficients found in almost every region (except square 9) were high, only squares 1, 3, 6 and 8 were correlated at 5% level of significance. This happens because only 3 monthly values were used for correlation calculations between the parameters. Nevertheless, it is still possible to see a clear tendency for

southern regions to have a higher negative correlation coefficient than northern regions.

Table 2 - Correlation coefficients (K) between SST inter-annual monthly mean and OC inter- annual monthly mean from 2002 to 2006 for the different regions. K critical value at 5% and 1% levels of significance respectively: 0,55 and 0,68.

Square	1	2	3	4	5	6	7	8	9
K	-0,87	-0,87	-0,90	-0,37	-0,94	-0,88	-0,85	-0,39	-0,53

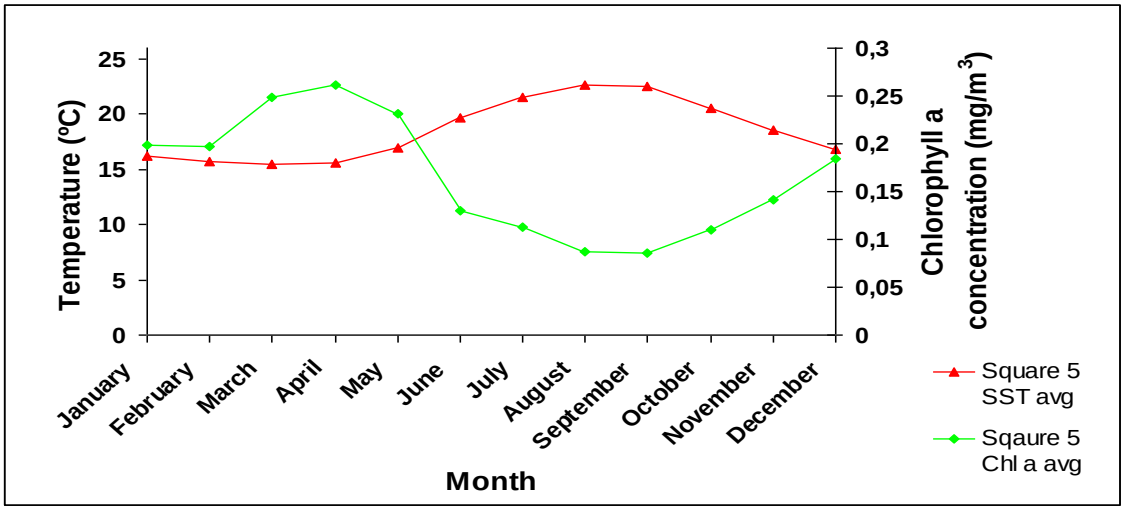

Figure 17 - AVHRR SST and MODIS OC inter-annual monthly means from 2002 to 2006 for square 5.

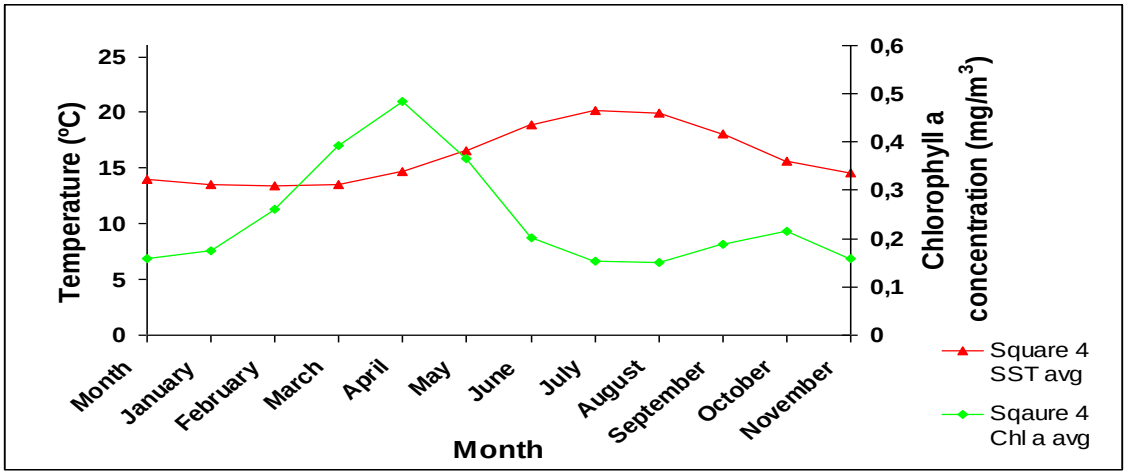

Figure 18 - AVHRR SST and MODIS OC inter-annual monthly means from 2002 to 2006 for square 5.

Table 3 - Correlation coefficients (K) between SST and OC during the period of spring bloom for the different regions. Years 2002 to 2006. K critical value at 5% and 1% levels of significance respectively: 0,95 and 0,99.

Square	1	2	3	4	5	6	7	8	9
K	-0,99	0,85	-0,99	0,86	-0,85	-0,98	-0,91	-0,97	-0,50

4.2.3.2. Inter-Annual Variability

Monthly SST and chlorophyll *a* means from July 2002 to December 2006 show a clear inverse relationship for each year of the studied period of time. As an example, Figure 19 shows evident inverse inter-annual seasonal cycle between SST and OC for square 6. In the graphic is also possible to see that to a comparatively high SST minimum in 2006 corresponds the lowest chlorophyll *a* peak during the winter-spring period.

In order to take out the seasonal cycle influence and enhance the inter-annual variability, anomalies of both SST and OC were calculated on a monthly basis. SST and OC monthly anomalies were then, independently, correlated throughout the years. The correlation coefficients (K) for each square are shown in Figure 20, Figure 21 and Figure 22 are graphical representations of Table 4. For better interpretation, they are separated into southern, northern and coastal areas, respectively. In southern regions it is possible to see a general tendency for parameters being more negatively correlated during the spring period (February to May), and to have lower or even positive correlation coefficients during summer, autumn and winter periods (June to January). For northern squares no clear trend is observed, with considerable variation of the correlation coefficients during the year and in all the squares. The coast of Portugal (square 8) has a general tendency to present some low positive coefficient values during winter and spring periods and negative coefficient values mainly during autumn. In the West African coast region (square 9) stronger negative correlation coefficients are present during spring (March to May), and autumn and winter (September to January) periods.

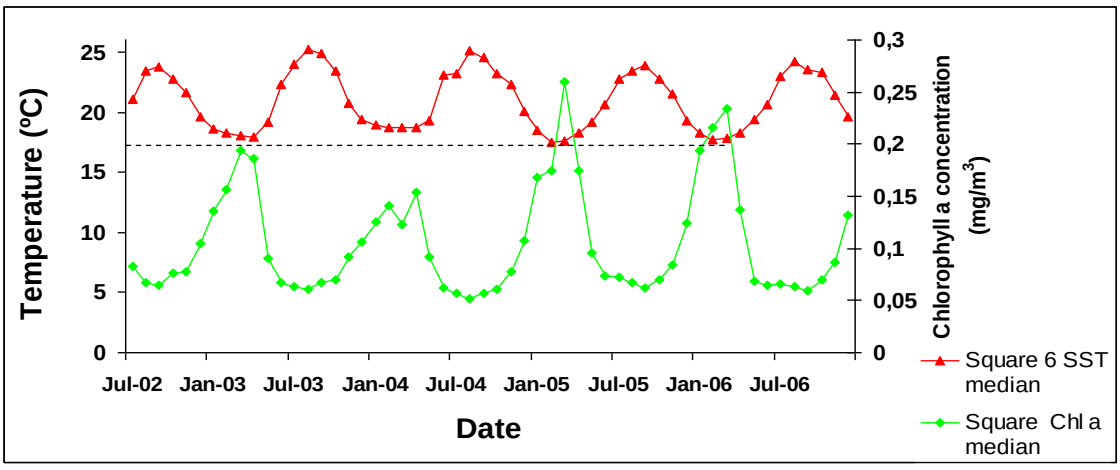

Figure 19 - AVHRR SST and MODIS OC monthly medians from July 2002 until December 2006 for square 6.

Table 4 - Correlation coefficients (K) between ΔSST monthly median and ΔOC monthly median from 2002 to 2006. K critical value at 5% and 1% levels of significance respectively: 0,81 and 0,92.

	Square 1	**Square 2**	**Square 3**	**Square 4**	**Square 5**	**Square 6**	**Square 7**	**Square 8**	**Square 9**
January	-0,24	-0,24	-0,99	0,56	0,38	-0,95	0,22	0,56	-0,87
February	-0,97	-0,32	-0,87	0,86	-0,01	-0,75	-0,90	0,53	0,75
March	-0,40	-1,00	-0,77	-0,73	0,86	-0,99	-0,90	0,81	-0,55
April	-0,98	0,58	-0,96	-0,28	0,79	-0,55	-0,96	0,19	-0,77
May	-0,73	-0,99	-0,94	0,43	0,81	-0,93	-0,28	0,48	-0,56
June	-0,59	-0,25	-0,66	-0,93	-0,87	-0,56	-0,50	-0,08	0,29
July	0,52	0,55	-0,36	-0,36	-0,95	-0,86	-0,42	-0,13	0,38
August	0,53	0,41	-0,16	-0,79	-0,30	-0,83	-0,67	-0,69	-0,25
September	0,40	0,40	-0,50	-0,84	-0,60	0,24	-0,89	-0,20	-0,58
October	-0,99	-0,83	-0,96	-0,96	-0,98	-0,52	0,30	-0,74	-0,43
November	-0,81	-0,81	0,53	-0,02	-0,79	-0,88	-0,73	-0,77	-0,65
December	0,08	-0,18	0,49	0,22	0,23	-0,30	-0,86	0,76	-0,42
K Annual mean	-0,348	-0,222	-0,513	-0,237	-0,121	-0,656	-0,550	0,059	-0,305

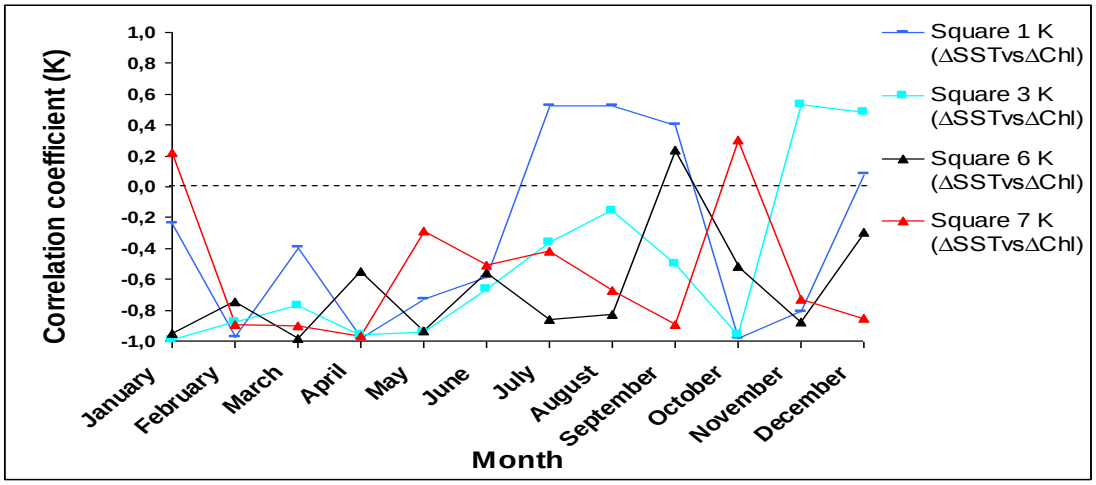

Figure 20 - Correlation coefficients (K) between ΔSST monthly mean and ΔOC monthly mean from 2002 to 2006 for southern regions.

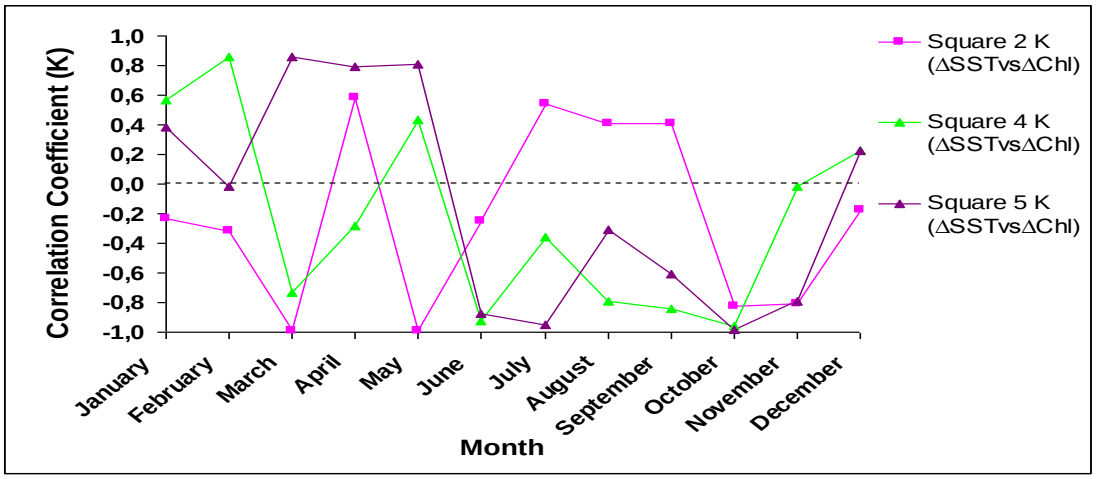

Figure 21 - Correlation coefficients (K) between ΔSST monthly mean and ΔOC monthly mean from 2002 to 2006 for northern regions.

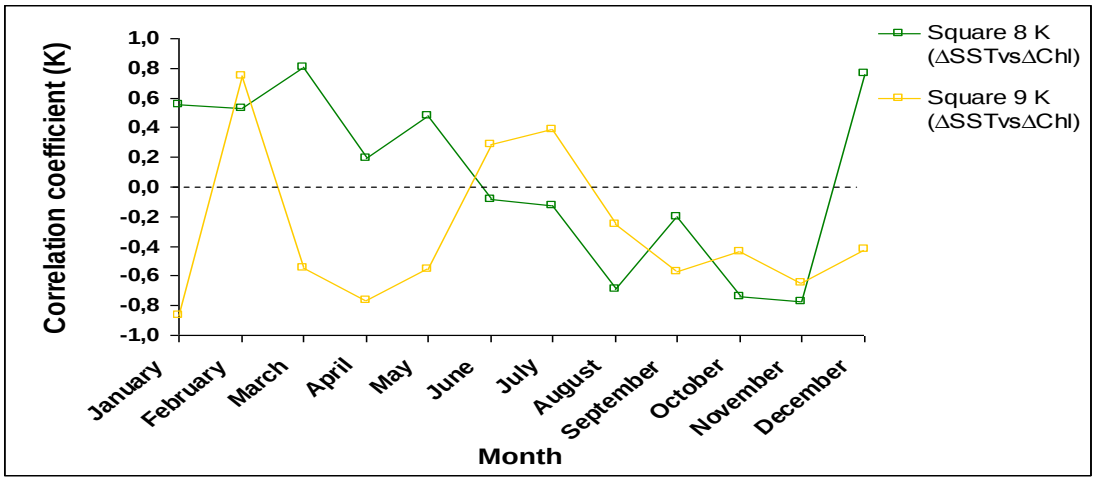

Figure 22 - Correlation coefficients (K) between ΔSST monthly median and ΔOC monthly median from 2002 to 2006 for coastal regions.

4.2.4 Variability of SST vs NAO

Some attempts were made to relate part of the observed SST inter-annual variability with the North Atlantic Oscillation (NAO). To do this, comparisons between the annual means of SST anomaly and NAO index were made. Figure 23 shows the results for the southern squares, where a similar pattern over the years is observed, with a fairly good level of correspondence between these two parameters in southern regions in 2003, 2004, 2005 and 2006. Year 2002 is somewhat different. Here high negative SST anomaly around -0.31/-0.47 was associated with lower, but still quite high and positive NAO index (0.04). The correspondence found between northern regions SST anomaly and NAO indexes on annual means was not very clear (Figure 24).

For the time interval (2002-2006), the correlation coefficient between the annual means SST anomalies and the NAO indexes was calculated. In spite of the good level of correspondence, no data was correlated at 5% level of significance. This possibly happens due to a very limited temporal scale, when only five annual means values were used. The corresponding correlation coefficients are presented in Table 5. Interestingly, the only two regions which showed a negative SST correlation with NAO where squares 2 and 4, both at the same latitude (latitude of the Azores region)

Some attempts were made to relate OC anomalies annual mean with NAO index annual mean, but correlations found were very low.

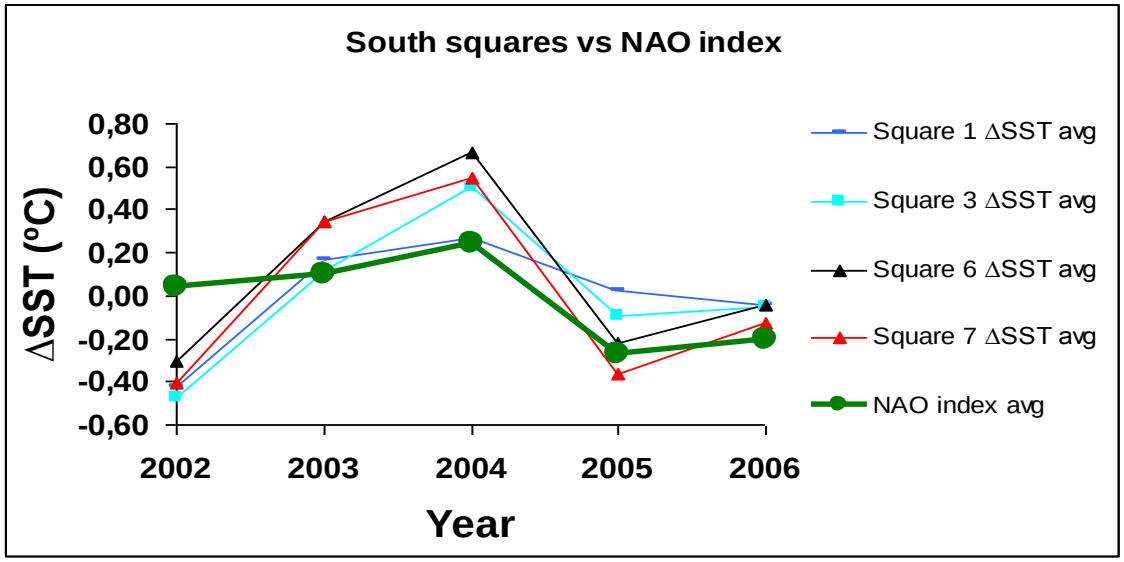

Figure 23 - SST annual mean anomaly versus annual mean NAO index from 2002 to 2006 for the southern squares.

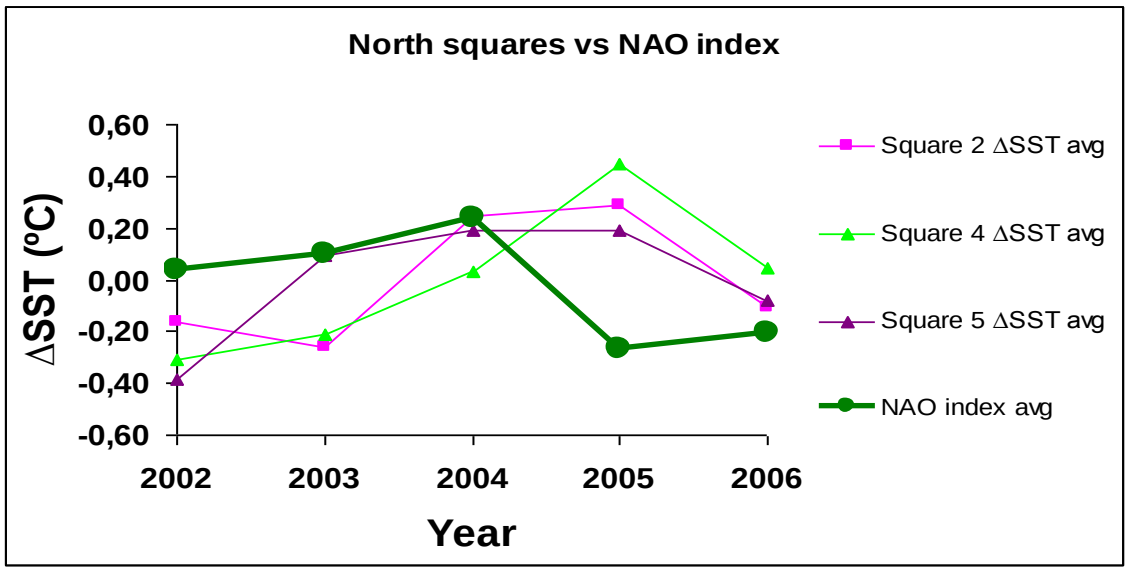

Figure 24 - SST anomaly annual mean and NAO index annual mean from 2002 to 2006 for northern regions.

Table 5 - Correlation coefficients between **ΔSST** anomaly annual mean and NAO index annual mean for the different regions. K critical value at 5% and 1% levels of significance respectively: 0,81 and 0,92.

Square	**1**	**2**	**3**	**4**	**5**	**6**	**7**
ΔSST vs NAO index correlation	0.30	-0.12	0.50	-0.62	0.03	0.74	0,75

5. DISCUSSION

In this chapter the results on SST and OC seasonal and inter-annual variability, obtained in the previous section, are discussed. Comparative analysis with some known physical processes and previous studies for the area are here addressed.

5.1. Seasonal Variability

At mid-latitudes, the temperature of the mixed layer is mainly a balance between solar heating tending to raise the temperature, and the stirring of the upper layers by wind which tends to mix the heat downwards, reducing the surface temperature and deepening the mixed layer (Robinson, 1985). The latent and sensible heat exchanges with atmosphere also play an important role at certain period of time. All these processes show strong seasonal variation, increasing from the tropics to mid-latitudes, thus, the upper ocean layer temperature shows a pronounced seasonal cycle.

Seasonal variability of solar heating resulted in SST gradients seasonal meridional migrations, in which enhanced SST advection during spring-summer seasons also seems to have played an important role. Martins *et al.* (2007) attributed this feature to seasonal Sub-tropical Gyre (SG) expansion. Our results also showed that for the whole study area strong SST seasonal patterns were evident. During all seasons meridional gradients were the most pronounced, with temperature increasing (decreasing) in southern (northern) latitudes, respectively. In winter, the low heat input and strong mixing by the winds results in lower temperatures and deeper upper mixed layer. In summer, the increased insolation and generally lower wind stirring, means that the shallow surface layer heats up, becoming thermally isolated (seasonal thermocline) from the deeper part of what was the winter mixed layer. Previous studies in the region also indicate that the upper layer water warming, and the associated isotherm displacement towards north during spring and early summer, is often accompanied by barring of the internal horizontal temperature patterns by formation of the seasonal thermocline (Bashmachnikov *et al.*, 2004, Martins *et al.*, 2007).

Apart of the meridional gradients, zonal isotherm tilt occurred creating a general SST pattern with NW-SE orientation and evident longitudinal gradients of SST during all

seasons. This was especially pronounced in summer and it is probably the reason why our westernmost region (square 1) presented the highest SST during summer. Zonal isotherm tilt during summertime suggests strong influence of the dominating eastward flow. Klein and Siedler (1989) found summer intensification of the eastward flow through the Azores from CTD data. Bashmachnikov *et al.* (2004) suggested that the pattern may be associated with lagged response of the Gulf Stream spring-early summer intensification or/and local forcing mechanisms, which increase the AzC transport in the late summer. Zonal orientation of SST gradients in the western part of the region are also enhanced due to the blocking effect of Midle-Atlantic Ridge (MAR) on the warm water transport to the eastern Atlantic basin (see, for example, Klein and Siedler, 1989).

Following Gould (1985) and based on *in-situ* temperature data retrieved from Argos buoys, Pingree *et al.* (1999) suggested associating the position of the Sub-Tropical Azores Front (AzF) with the 18ºC isotherm during cold season. Similar to the results of Bashmachnikov *et al.* (2004), our results show that, during wintertime, the AzF if identified at the position of the 18ºC isotherm was located south of 34-35ºN. The observed seasonal migrations of the AzC main jet (south retreat in summer and progress northward in winter), the earlier (spring) exhibit of similar seasonal pattern of the Gulf Stream, and the analogous seasonal variability of the North Equatorial current, all of these reflect in fact the meridional seasonal migrations and transport variability of the North Atlantic SG (Stramma and Siedler, 1988). The seasonal SST variability over the Sub-Tropical NE Atlantic is sensibly affected by the transport changes described above.

Coastal regions (squares 8 and 9) have a distinct seasonal pattern. The mean temperature rose during early spring and kept more or less stable during summer time. In contrast with oceanic regions, which have typical SST maximum in August, for the coastal regions the summer maximum was not that clearly pronounced. Nevertheless, results for west Portuguese coast (square 8) are consistent with previous results by Matzen (2004) which registered higher surface temperature during summer period. Oliveira *et al.* (2008) showed that the summer oceanographic conditions along the west Portuguese coast are dominated by coastal upwelling driven by persistent equatorward winds. Associated filaments, previously described by Sousa and Bricaud

(1992), Matzen (2004) and Oliveira *et al.* (2008) propagate offshore and cause relatively high spatial-temporal variability resulting in a wide band of cooler water at the coast. The same authors showed that the upwelling intensity in the Portuguese coast is maximum during the months of July-September. For the same period, Barton *et al.* (1998) reported an increase of northern winds over the West African coast and respective Canary upwelling intensification. This intensification can be seen in our results for the West African coast (square 9), where, although having typical summer maximum, the temperature difference with the oceanic region (square 7) is about 2ºC in winter and 3^{o}C in summer.

The abundance of phytoplankton in water mass is believed to represent a balance between the processes of growth (photosynthesis) and mortality (including grazing). The production processes are controlled mainly by the abundance of light and nutrients. The seasonal change in growth is closely tied to the change in the depth of the mixed layer relative to the depth of photic layer, both of which, in turn, are regulated by climatological processes such as wind stress, air-sea temperature exchange and changes in solar radiation intensity (Yentsch, 1993).

The chlorophyll concentration at the sea surface generally responds to the seasonal cycle of solar heating that strongly impacts vertical stability, which regulates the intensity of upward nutrient flux (Dandonneau *et al.*, 2004). Results show a general tendency of the mean chlorophyll *a* to decrease towards southern latitudes, where permanently stratified oligotrophic Sub-Tropical waters are found. The dominant scheme is a transition from a high-latitude system where the bloom is triggered by the rapid temperature, light and vertical stability increase in spring, to a low-latitude system where it is triggered by episodic weakening of vertical stability that allows deeper nutrients to fuel the permanently warm, nutrient-exhausted mixed layer (Dandonneau *et al.*, 2004).

In the northern part of the study region (squares 2, 4 and 5) a typical mid-latitude seasonal curve with pronounced spring (usually May) bloom is found. These blooms happen when warmer temperature and increased sunlight, creates a pycnocline that traps nutrients at the ocean surface. During summertime, phytoplankton uses up the available nutrients which are gradually depleted in the upper layer due to animal's death and sink down to the deeper layers. In autumn, cooler days cause some vertical

mixing that may bring nutrients up from below resulting in a relatively smaller fall bloom (Martins *et al.*, 2007). In our results, fall bloom was present only in squares 2 and 4. Once winter begins, decreasing surface temperature and frequent storms cause heavy mixing. As phytoplankton do not remain most of the time in the photic layer, the sunlight becomes a limiting factor and winter is characterized by relatively stable low-biomass conditions at these latitudes (Sverdrup, 1953).

More southern regions (squares 1, 3, 6 and 7), located at the northern border of the SG, present a different seasonal pattern with a reduced winter-spring bloom and maximum chlorophyll *a* values to occur in late winter - early spring (usually March). Here, in the more equatorward provinces of the Westerlies, the consistent feature of the seasonal cycle is that algal biomass accumulates only during the first few months of the progressive increase in primary production rate during winter (Longhurst, 1995). Some months before the spring production maximum, a late winter chlorophyll maximum is reached and biomass declines progressively towards a late summer minimum. During the winter months, the area of the oligotrophic gyre is smaller compared to the summer months because winter storms and stronger winter winds increase vertical mixing in the subtropical regions (Polovina *et al.*, 2008). At these latitudes cooling and wind stress during autumn period is not enough to mix the water and bring the nutrients to the strongly stratified photic layer, so no autumn bloom occurs.

Within these oligotrophic regimes, the presence of mesoscale features such as fronts, eddies and seamounts represents important inputs of nutrient to photic layer, leading to increases in biological production, favoring export production and the prevalence of short food webs. (Huskin *et al.*, 2001). Our results showed that mean surface chlorophyll *a* values for sub-tropical regions were low in summer (<0.1 mg/m^3) but increased in the cooling period reaching values of 0.25 mg/m^3 in late March. Based on cruise data near 34ºN in the Eastern Basin, Pingree *et al.*(1999) found very similar surface values (<0.1 mg/m^3 for summer and 0.3 mg/m^3 for March). Chlorophyll spring bloom values for square 3 are slightly higher when comparing with squares 1 and 6, this possible reflects entrainment of northerly richer waters due to the meandering of the AzC just west of the area. Significantly higher concentrations in temperate regions

(square 4) than sub-tropical and tropical ones, was mainly due to the stronger spring bloom, which extends from 39º to 50ºN (Longhurst, 1995 and E. Teira *et al*. 2005).

Coastal areas (squares 8 and 9) showed a completely distinct seasonal pattern than the oceanic regions. At the Portuguese coast (square 8) chlorophyll *a* concentration increased sharply during late winter reaching its maximum in early spring (March). Then chlorophyll *a* decreased, but another pronounced bloom occurred in summer, with mean concentration values reaching 0.99 mg/m^3 by August. This pronounced summer bloom is due to the intensification of the coastal upwelling driven by stronger trade winds, being also more aligned with the coast. This summer bloom was previously reported by Sousa and Bricaud (1992), and Oliveira *et al.* (2008). Seasonal variability in square 9 (West African coastal region) had no clear defined seasonal cycle, having with more or less stable chlorophyll concentration over the year (~0.4 mg/m^3), although, the chlorophyll *a* tended to slightly increase in spring. Low mean chlorophyll values through the whole year around ~0.5 mg/m^3 with a slight spring increase were also reported by Barton *et al.* (1998). The relatively small year round variation in chlorophyll concentrations integrated over the water column contrasts with the much larger variability in primary production. During the autumn, primary production is as low as in the most oligotrophic regions of the world. In late winter and early spring, however, productivity values increase more than an order of magnitude. The seasonal increase in primary productivity is not accompanied by a similar increase in chlorophyll accumulation. Barton *et al.* (1998), based on *in situ* chlorophyll data together with the complete archive of CZCS images for the Canaries region, indicated that at the start of the mixing period (January–February) only a weak bloom is produced. It appears that grazers take advantage of the phytoplankton bloom rapidly to prevent any surface accumulation (Arístegui, 1990 *fidé* Barton *et al.,* 1998), so that the bloom never has time to build up and then weakens into spring and summer. Zooplankton biomass reaches its maximum a few weeks after the phytoplankton peak, and drops sharply as the algal standing crop falls (Barton *et al.,* 1998).

5.2. Inter-Annual Variability

Over the middle and high latitudes of the Northern Hemispheric the most prominent and recurrent pattern of atmospheric variability is the North Atlantic Oscillation (NAO) (Talley, 1996**,** Hurrel *et al.*, 2003 and Visbeck *et al.*, 2003). Since mid-latitude SST is mainly governed by the atmospheric forcing (Chen *et al.*, 2002), NAO is probably the main source of inter-annual variability of SST in the region. NAO refers to swings in the atmospheric sea level pressure difference between the Artic (normally Iceland) and the sub-tropical Atlantic (Azores) that is most noticeable during the boreal cold season (November-April) and is associated with changes in the mean wind speed and direction. Significant changes in the ocean currents and their related heat transport are also induced by changes in the NAO (Hurrel *et al.*, 2003). It has long been recognized that fluctuations in SST and the strength of the NAO are related, and there are clear indications that the North Atlantic Ocean varies significantly with the overlying atmosphere. Visbeck *et al.*, (2003) describe in detail the oceanic response to NAO variability. This author suggests that the SST anomalies are driven by changes in the surface wind and air-sea heat exchanges associated with NAO variations. The relationship is strongest when the NAO index leads an index of the SST variability by several weeks, which highlights the well-known result that large-scale SST over the extra-tropical oceans responds to atmospheric forcing on monthly and seasonal time scales (Hurrel *et al.*, 2003).

Our results for the correlations between annual SST anomalies and annual NAO index value for oceanic regions, show higher correlation in the southern regions (squares 1, 3, 6 and 7) as compared with the northern ones (squares 2, 4 and 5). Positive and increasing SST anomalies were found during the years of 2003 and 2004 responding to a slightly positive and also increasing NAO index in the same years. An possible explanation could be related to the fact that the anticyclonic circulation intensity of the Sub-Tropical Gyre (SG) is also correlated with NAO variations (Hurrel *et al.*, 2003). When the NAO index is positive, enhanced westerly flow across the North Atlantic forces clockwise intensification of the SG around the sub-tropical Atlantic high-pressure center (Hurrel *et al.*, 2003), which brings warmer water to the region from the Western Atlantic basin. The enhanced surface winds also promote an accumulation

of warmer surface waters in the SG, which can also enhance the positive correlations. Since the southern squares are located in the sub-tropical region they get much stronger signal from variations in the NAO index.

NAO variability influences abundance, biomass, distribution, growth rates and survival rates of the organisms (Drinkwater *et al.*, 2003). The impacts of NAO are generally mediated through local changes in the physical environment, such as winds, ocean temperatures and circulation patterns (Drinkwater *et al.*, 2003). It is known that inter-annual variability of both phytoplankton and zooplankton reflects changes in winds and ocean temperatures. Given the importance of vertical mixing and stratification in both timing of the spring bloom and the succession of the phytoplankton species, it is expected that NAO might be linked to inter-annual variability in primary production through its relationship to winds and air temperatures (Drinkwater *et al.*, 2003). It is important to notice that the biology is not responding directly to the NAO but rather indirectly through changes in the local physical or chemical characteristics of the water that are themselves associated with variability in the NAO.

6. CONCLUSIONS

Main objectives of this work were to study temporal and spatial variability of SST and OC in the Sub-tropical NE Atlantic, and to find statistical dependencies between their patterns and sign of their temporal changes on monthly, seasonal and inter-annual scales. For a period of five years, AVHRR (SST) and MODIS (OC) monthly data obtained from the Physical Oceanography Distributed Active Archive Center (PO.DAAC) and "Ocean Color Level 3 browser" respectively, was used to compute seasonal and annual medians within the study area. For further statistical analysis, nine sub-regions, distributed over the whole area, were defined.

Results for the SST field suggest distinct inter-annual seasonal cycle with seasonal warming clearly evident in all regions initiating during winter-spring and cooling during summer-autumn months. Isotherm tilt during summer period should be related with the stabilizing of the Azores Anti-cyclone in the south-western part of the region, creating a strong and stable thermocline. Stronger advection of warm waters from Sargasso Sea in summer is adding to a related SST increase. NOAA Wind data shows that Trade Winds in sub-region 7 are increasing during summer, this is probably the reason why this region gets lower SST values during this season reaching a maximum late in September.

Coastal regions showed somewhat distinct seasonal pattern. Seasonal temperature amplitudes were lower because despite the increase in solar hitting during summer, the wind related intensification of the coastal upwelling did not permitted a significant temperature increase.

Results also show that chlorophyll *a*, generally decreased towards southern latitudes, resulting from a gradual transition from more productive Eastern North Atlantic waters to stratified oligotrophic tropical waters. The OC field suggested distinct seasonal cycle with a transition from a mid-latitude system with pronounced spring bloom triggered by formation of seasonal thermocline, to a tropical system where the bloom it is triggered, in late winter, by less vertical stability in the upper layer allowing deeper nutrients to fuel the permanently warm and nutrient-exhausted mixed layer. Sub-tropical sub-regions 2 and 5 had higher inter-annual variability and seemed to be more sensible to weather conditions. Comparing to oceanic regions, the

coastal ones presented higher mean chlorophyll values and, at the coast of Portugal a strong summer bloom was present, this was mainly due to intensification of coastal upwelling as a result of increase in Trade Wind speed in summer. At the West African coast chlorophyll *a* concentration stayed more a less stable over the whole year.

A clear inverse relationship between surface temperatures and chlorophyll *a* distributions was found in subtropical and tropical regions. Increased pigment concentration is generally associated with lower temperature values. The relationship was not pronounced in most northern and coastal regions. In square 4 there was no winter chlorophyll increase so this means that the winter mixing has a negative effect here. SST and OC in tropical regions have higher negative correlation during spring and summer suggesting that the dependencies change with seasons.

Results show that, on inter-annual time scales, NAO has some influence over the physical processes in the tropical area. Particularly we found strong negative correlations between SST and NAO index.

In conclusion, coupled inter-annual and seasonal variability are clearly highlighted in the SST and OC imagery, providing relevant information to study ocean dynamics variability within the Sub-Tropical NE Atlantic. Our study shows that intensity of wind mixing has an important impact on the chlorophyll concentration in the region. However, for a better understanding of regional to large scale influences in the region, it is important that further studies combining multi-sensor data sets from different satellites and *in situ* data are made.

7. ACKNOWLEDGEMENTS

I am very grateful to my advisors, Dr. Igor Bashmachnikov and Prof. Ana Martins for all their attention and dedication. In particular, I would like to thank Dr. Bashmachnikov for the great help it gave me along the way, through interesting physical oceanography lessons, and also by initiating me on MatLab programming, providing me the initial programs framework for this work.

I am thankful to Prof. João Gonçalves, Dr. Igor Bashmachnikov, Prof. Ana Martins and Dr. Paolo Lambardi for accepting to become part of my dissertation committee.

I am grateful to all my colleagues at the Section of Oceanography at the Department of Oceanography and Fisheries (DOP/UAç) for all the help they gave me during the development of this research. In particular, I would like to thank Guilherme Lopes for the great help on improving initial MatLab programs.

I thank the PO.DAAC and MODIS Ocean Color Web centers for providing freely on the web the data sets used in this study.

I thank the staff at the University of the Azores and in particular at the Department of Oceanography and Fisheries (DOP/UAç) for their administrative and logistic help along the way.

Computer resources and facilities were provided by the Department of Oceanography and Fisheries at the University of the Azores. This support is greatly acknowledged.

I am very much grateful to all my family and friends for all their support along the way. In particular I want to thank my university friends: Adriano, Cátia, Clara, Joana, Laura, Margarida, Nuno, Parra, Paulo, Pedro, Tiago and Tiago Caroxo.

Above all, I want to thank Ana.

8. REFERENCES

Barnes, W. L., T. S. Pagano & V. Salomonson, 1998: Prelaunch characteristics of the moderate resolution imaging spectroradiometer (MODIS) on EOS-AMI. IEEE Trans. Geosci. *Remote Sensing*, **36** (4), 1088–1100.

Barton, I. J. & R. P. Cechet, 1989: Comparison and optimization of AVHRR sea surface temperature algorithms. *Journal of Atmospheric and Oceanic Technology* **6**, 1083–1089.

Barton, E.D., J. Arístegui, P. Tett, M. Cantón, J. Garcı´a-Braune, S. Hernández-León, L. Nykjaer, C. Almeida, J. Almunia, S. Ballesteros, G. Basterretxea, J. Escánez, L. García-Weill, A. Herna´ndez-Guerra, F. López-Laatzen, R. Molina, M.F. Montero, E. Navarro-Pérez, J.M. Rodríguez, K. van Lenning, H. Vélez & K. Wild, 1998: The transition zone of the Canary Current upwelling region. Progress in Oceanography, **41,** 455–504.

Bashmachnikov,I., V. Lafon & A. Martins, 2004: Sea surface Temperature Distribution in the Azores Region. Part II: Space-Time Variability and Underlying Mechanisms. *Arquipélago.* Life and Marine Sciences, **21**A, 19-32.

Brown, J. W., O. B. Brown & R. H. Evans, 1993: Calibration of AVHRR Infrared channels: a new approach to non-linear correction*, Journal of Geophysical Research*, **98** (NC10), 18257-18268.

Clarke G. L., G. C. Ewing & C. J. Lorenzen, 1970: Spectra of backscattered light from sea obtained from aircraft as a measure of chlorophyll concentration. *Science,* **16**, 1119–21.

Dandonneau, Y., P. I. Deschamps, J. M. Nicolas, H. Loisel, J. Blanchot, Y. Montel, F. Thieuleux & G. Bécu, 2004 : Seasonal and interannual variability of ocean color and

composition of phytoplankton communities in the North Atlantic, equatorial Pacific and South Pacific. *Deep-Sea Research II*, **51**, 303–318.

Donlon, C. J., P. J. Minett, C. Gentemann, T. J. Nightingale, I. J. Barton, B. Ward & M. J. Murray, 2002: Toward Improved Validation of Satellite Sea Surface Skin Temperature Measurements for Climate Research. *Journal of Climate*, **15**, 353-369.

Drinkwater, K. F., A. Belgrano, A. Borja, A. Conversi, M. Edwards, C. H. Greene, G. Ottersen, A. J. Pershing & H. Walker, 2003: The response of Marine Ecosystems to Climate Variability Associated With the North Atlantic Oscillation In: The North Atlantic Oscillation: Climatic Significance and Environmental Impact. *American Geophysical Union*, **134.**

Emery, W. J., G. A. Wick & P. Schluessel. 1995: Skin and Bulk Sea Surface Temperatures: Satellite Measurement and Corrections In: M. Ikeda and F. W. Dobson. Oceanographic Applications of Remote Sensing.

Emery, W. J., S. Castro, G. A. Wick, P. Schluessel & C. J. Donlon, 2001: Estimating Sea Surface Temperature From Infrared Satellite and In situ Temperature Data. *Bulletin of the American Meteorological Society*, **82**, 12, 2773-2786

Evans, R. & G. Podestá, 1998: Pathfinder Sea Surface Temperature Algorithm. *University of Miami, Rosenstiel, School of Marine and Atmospheric Science.*

Fox, M. F., D. R. Kester & J. A. Yoder, 2005: Spatial and Temporal Distributions of Surface Temperature and Chlorophyll in the Gulf of Maine During 1998 Using SeaWiFS and AVHRR Imagery. *Marine Chemistry*, **97**, 104-123.

Gentemann, C. L., C. J. Donlon, A. S. Meneth & F. J. Wentz, 2003: Diurnal signals in satellite sea surface temperature measurements. *Geophysical research letters*, **30,** (N3): 1140.

Gould, W. J., 1985: Physical oceanography of the Azores front. *Progress in Oceanography,* **14**, 167-190.

Gower, J., K. L. Denman & R. J. Holyer, 1980: Phytoplankton patchiness indicates the fluctuation spectrum of mesoscale oceanic structure. *Nature,* **288**, 157-159.

Hurrel, J. W., Y. Kushnir, G. Ottersen & M. Visbeck, 2003: An Overview of the North Atlantic Oscillation. *Geophysical Monograph,* **134**, 10.1029/134GM01.

Huskin, I., R. Anadón, G. Medina, R. N. Head & R. P. Harris, 2001: Mesozooplankton distribution and copepod grazing in the Subtropical Atlantic near the Azores: Influence of mesoscale structures. *Journal of Plankton research*, **23**, 7, 671-691.

Klein, B. & G. Siedler, 1989: On the origin of the Azores current. *Journal of Geophysical Reseach,* **94** (C5), 6159-6168.

Lafon, V., A. Martins, M. Figueiredo, M. A. Melo Rodrigues, I. Bashmachnikov, A. Mendonça, L. Macedo & N. Goulart, 2004: Sea Surface Temperature Distribution in the Azores Region. Part: I: AVHRR Imagery and *In Situ* Data Processing. *Arquipélago. Life and Marine Sciences*, **21**A, 1-18.

Lewis, M. R., 1995: Coastal Zone Color Scanner on Nimbus and Sea-Viewing Wide Field-of-View Sensor on Seastar In: M. Ikeda and F. W. Dobson. Oceanographic Applications of Remote Sensing.

Longhurst, A.R., 1995: Seasonal Cycles of Pelagic Production and Consumption. *Progress in Oceanography*, **36**, 2, 77-167.

Martins, A. M., A. S. B. Amorim, M. P. Figueiredo, R. J. Sousa, A. Mendonça, I.Bashmachnikov & D. S. Carvalho, 2007: Sea Surface Temperature (AVHRR, MODIS) and Ocean Colour (MODIS) seasonal and interannual variability in the

Macaronesian islands of Azores, Madeira, and Canaries. *Proceedings of SPIE,* 6743, 15.

Matzen, J., 2004: Caracterização qualitative do fenómeno de afloramento costeiro de Verão na Região de Aveiro. Universidade de Aveiro, departamento de Física. 158pp.

McClain, C. R., 2008: A Decade of Satellite Ocean Color Observations. *Annual Review of Marine Science*, **1**, 19-42.

McClain, E. P., W. G. Pichel & C. C. Walton, 1985: Comparative performance AVHRR-based multichannel sea surface temperatures, *Journal of Geophysical Research*, **90**, 11,587-11,601.

McClain, C. R., S. R. Signorini & J. R. Christian, 2004: Subtropical gyre variability observed by ocean-color satellites, *Deep Sea Research*, Part II, **51**, 281– 301.

McGillicuddy, D. J., V. K. Kosnyrev, J. P. Ryan & J. A. Yoder, 2001: Covariation of mesoscale ocean color and sea-surface temperature patterns in the Sargasso *Sea. Deep-Sea Research II*, **48,** 1823-1836.

Minnett, P. J. 1990: The regional optimization of infrared measurements of sea-surface temperature from space. *Journal of Geophysical Research,* **95,** 13 497–13 510.

Moliner, G. G. & J. A. Yoder, 1994: Variability in pigment concentration in warm-core rings as determined by coastal zone color scanner satellite imagery from the Mid-Atlantic Bight. *Journal of Geophysical Research*. **99**, 14277-14290.

Oliveira, P. B., R. Nolasco, J. Dubert, T. Moita & A. Peliz, 2008: Surface temperature, chlorophyll and advection patterns during a summer upwelling event off central Portugal. Continental Shelf Research, *in press*.

Pingree, R.D., C. Garcia-Soto & B. Sinha, 1999: Position and structure of the Subtropical/Azores front region from combined Lagrangian and remote sensing (IR/altimiter/SeaWiFS)measurements. *Journal of the Marine Biological Association of the UK,* **79**, 769-792.

Polovina, J. J., E. A. Howell & M. Abecassis, 2008: Ocean's least productive waters are expanding. *Geophys. Res. Lett.* **35**,L03618.

Robinson, I. S., 1985: Visible wavelength "ocean-colour" sensors In: Ellis Horwood limited. Satellite Oceanography: an introduction for oceanographers and remote-sensing scientists.

Salomonson, V., B. Guenther & E. Masuoka, 2001: A summary of the status of the EOS Terra Mission Moderate Resolution Imaging Spectroradiometer (MODIS) and attendant data product development after one year of on-orbit performance. *Proceedings of the International Geoscience and Remote Sensing Symposium*/ IGARSS'2001, Sydney, Australia, 9–13.

Savtchenko, A., D. Ouzounov, S. Ahmad, J. Acker, G. Leptoukh, J. Koziana & D. Nickless, 2004: Terra and Aqua MODIS products available from NASA GES DAAC. *Advances in space Research*, **34**, 710-714.

Sousa, F. M. & A. Bricaud, 1992: Satellite-Derived Phytoplankton Pigment Structures in the Portuguese Upwelling Area. *Journal of Geophysical research*, 97, c7, 11343-11356.

Stramma, L. & G. Siedler, 1988: Seasonal changes in the North Atlantic subtropical gyre. *Journal of Geophysical Research,* **93** (C7): 8111-8118.

Sverdrup, H. U., 1953: On the conditions for the vernal blooming of phytoplankton. *Journal du Conseil Perm. International pour l'Exploration de la Mer,* **18**, 287-295.

Talley, L. D., 1996: North Atlantic circulation and variability, reviewed for the CNLS conference. *Physica D*, **98**, 625-646.

Teira, E., B. Mouriño, E. Marañón, V. Pérez, M. J. Pazó, P. Serret, D. de Armas, J. Escánez, E. M. Woodward & E. Fernández, 2005: Variability of chlorophyll and primary production in the Eastern North Atlantic Subtropical Gyre: potential factors affecting phytoplankton activity. *Deep-Sea Research I*, **52**, 569–588.

Vazquez, J., E. Kearns & K. Casey, 1998: NOAA/NASA AVHRR Oceans Pathfinder Sea Surface Temperature Data Set User's Reference Manual Version 4.0. *JPL Publication,* D-14070

Visbeck, M., E. P. Chassignet, R. G. Curry, T. L. Delworth, R. R. Dickson & G. Krahmann, 2003: The ocean's Response to North Atlantic Oscillation Variability In: The North Atlantic Oscillation, Climate Significance and Environmental Impact.

Yentsch, C. S., 1993: CZCS: Its role in the study of growth of oceanic phytoplankton In: Ocean Colour: Theory an Applications in a Decade of CZCS Experience, *Kluwer Academic Publishers.*

Electronic Reference

Climate Prediction Center, 2008: North Atlantic Oscillation. *In:* http://www.cpc.ncep.noaa.gov/products/precip/CWlink/pna/nao.shtml (Last access October 21, 2008);

GHRSST-PP, 2005: Understanding Sea Surface Temperature. *In*: http://ghrsst-pp.metoffice.com/pages/sst_definitions/ (Last accessed June 13, 2008).

PODAAC, Physical Oceanography DAAC, 2008: Mission *In*: http://podaac.jpl.nasa.gov/DATA_CATALOG/avhrrinfo.html (Last accessed May 25, 2008).

AVHRR Pathfinder Oceans, 2000: Matchup Database 1985-1997 (Version 19.0). *In*: http://www.rsmas.miami.edu/groups/rrsl/pathfinder/Matchups/match_index.html (Las access September 3, 2008).

Ocean Color Documents, 2008: Overview of MODIS Aqua Data Processing and Distribution. *In*: http://oceancolor.gsfc.nasa.gov/DOCS/MODISA_processing.html (Last access September 9, 2008).